

SPERRVERMERK/CLAUSE OF CONFIDENTIALITY

Auf Wunsch der Firma/Institution / upon request of:

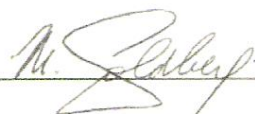
Michael Goldberg

ist die vorliegende Masterarbeit für die angegebene Dauer von maximal 5 Jahren für die öffentliche Nutzung zu sperren/will the present master thesis be retained from public access for the period of max.5 years

Dauer der Sperre / period: 2 Jahre /years

Veröffentlichung, Vervielfältigung und Einsichtnahme sind ohne ausdrückliche Genehmigung der o.a. Firma und des Verfassers/der Verfasserin bis zum genannten Datum nicht gestattet/*Unauthorized reading, publication and duplication will not be allowed without explicit consent given by the above-mentioned company and the author before:*

zu veröffentlichen am/publication allowed: 13/02/18

Unterschrift/Signature: 

Name/Funktion. Name/position: Michael Goldberg/Assistant Professor

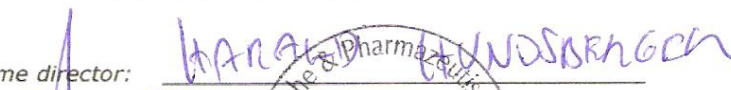
Firma /Firmenstempel/Company/Seal:

~~~~~

VerfasserIn Masterarbeit/Author master thesis: DELORIA, Abigail Joyce B.Sc.

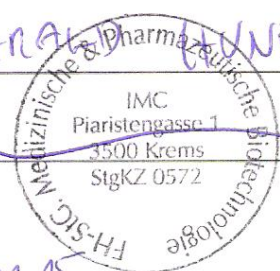
Unterschrift/Signature: 

~~~~~

Studiengangsleiter /Programme director: 

Unterschrift/Signature: _____

Stempel FH/ Seal:



Bestätigt am: /Notified as of: 12.01.18

mRNA in the Loop:
Circular mRNA as a Novel template for
Therapeutic Gene Transfer

submitted at the

Austrian Marshall Plan Foundation



AUSTRIAN
MARSHALL PLAN FOUNDATION
VIENNA | AUSTRIA

by

Abigail Joyce DELORIA

Area of Emphasis:

Gene Therapy, Master's Internship at the Dana-Farber Cancer Institute/Harvard Medical school, Boston, MA, USA.

Master's Program: Medical and Pharmaceutical Biotechnology, IMC FH Krems

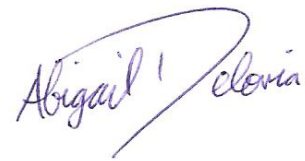
External Supervisor: Michael Goldberg PhD (PI)

Internal Supervisor: Priv.Doiz. Dr. Reinhard Klein

Statutory Declaration

"I declare in lieu of an oath that I have written this master thesis myself and that I have not used any sources or resources other than stated for its preparation. I further declare that I have clearly indicated all direct and indirect quotations. This master thesis has not been submitted elsewhere for examination purposes."

Date: April 22nd , 2016

A handwritten signature in blue ink that reads "Abigail Joyceloria". The signature is written in a cursive style with a large, sweeping flourish over the name.

Abigail Joyce DELORIA

SPERRVERMERK/CLAUSE OF CONFIDENTIALITY

Auf Wunsch der Firma/Institution / upon request of:

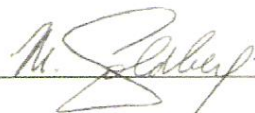
Michael Goldberg

ist die vorliegende Masterarbeit für die angegebene Dauer von maximal 5 Jahren für die öffentliche Nutzung zu sperren/will the present master thesis be retained from public access for the period of max.5 years

Dauer der Sperre / period: 2 Jahre /years

Veröffentlichung, Vervielfältigung und Einsichtnahme sind ohne ausdrückliche Genehmigung der o.a. Firma und des Verfassers/der Verfasserin bis zum genannten Datum nicht gestattet/Unauthorized reading, publication and duplication will not be allowed without explicit consent given by the above-mentioned company and the author before:

zu veröffentlichen am/publication allowed: 13/02/18

Unterschrift/Signature: 

Name/Funktion. Name/position: Michael Goldberg/Assistant Professor

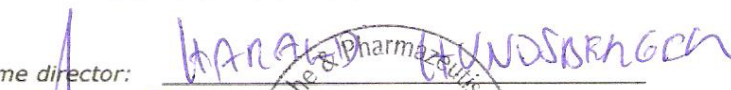
Firma /Firmenstempel/Company/Seal:

~~~~~

VerfasserIn Masterarbeit/Author master thesis: DELORIA, Abigail Joyce B.Sc.

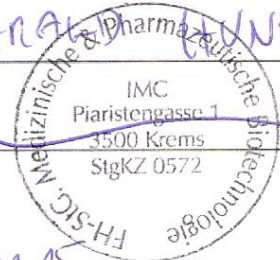
Unterschrift/Signature: 

~~~~~

Studiengangleiter /Programme director: 

Unterschrift/Signature: _____

Stempel FH/ Seal:



Bestätigt am: /Notified as of: 12.01.18

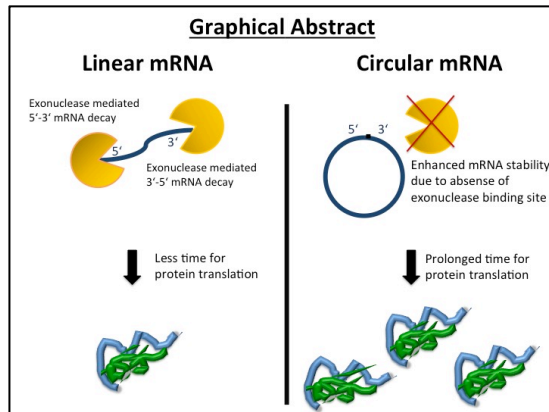
Acknowledgements

I would like to thank the Marshall Plan Foundation for financially supporting me during my internship in Boston, USA. Furthermore, I would like to express my deep gratitude to PI Dr. Michael Goldberg at the Dana-Farber Cancer Institute/Harvard Medical School for giving me the opportunity to learn from him and his thriving, likewise inspiring, team (PhD candidate C. Hartl, Dr. D. Schmid, Dr. S. Mohinta, Dr. V. Greiner, Dr. C. Park, Master student N. Subedi). Thereby, I would in particular like to highlight and thank PhD candidate Ellese Carmona for letting me participate in her project and for her scientific guidance. I am also grateful for all the assistance I obtained from the Department of Cancer Immunology and Virology which the laboratory is part of, especially Dr. A. Cartwright and Dr. J. Leavenworth.

Moreover, I would also like to thank the whole IMC University of Applied Sciences Krems team, my internal supervisor Priv. Doz. Dr. Reinhard Klein, and the rector Prof. (FH) Mag. Eva Werner, hon. Prof. for making my scientific career endeavor possible.

Last but not least I thank my family and friends for all their support.

Abstract



Mutated or missing proteins commonly contribute to the development of several formidable diseases, such as cancer and type I diabetes. To replace these malfunctioning proteins, gene therapy in particular the use of messenger (m)RNA, bears a great potential. However, mRNA is prone to degradation. Thus, we sought

to examine whether circular mRNA can escape rapid degradation in comparison to canonical linear mRNA and, consequently, exhibit enhanced stability with a resultant prolongation of protein expression. To our knowledge, this is the first work to use circular mRNA as a possible therapeutic option.

In our murine *in vivo* studies, we used an mRNA reporter construct encoding nanoluciferase (Nluc) and 3xFlag-tag to test the aforementioned hypothesis. In contrast to linear mRNA, *in vivo* imaging system (IVIS) data indicated a positive trend of Nluc-protein expression during a time course of 4 to 8 hours. Further, analyses of mRNA levels in murine liver demonstrated that circular mRNA was present 3-fold higher than linear mRNA over a 3-day time course study. Likewise, circular mRNA remains resistant to degradation, demonstrated by a 68% loss in linear mRNA, compared to only 18% of circular mRNA.

In conclusion, these studies suggest that circular mRNA compared to linear structures enhance nucleic acid stability and is associated with prolonged protein translation in murine liver. Therefore, circular mRNA is a promising therapeutic contender and would enhance future development and application of mRNA therapy, providing an improved benefit to disease management.

Keywords: mRNA, gene therapy, *in vivo* study, pharmacokinetic

Table of Contents

Statutory Declaration	1
Acknowledgements.....	3
Abstract.....	4
Table of Contents	5
List of Tables and Figures	8
List of Abbreviations.....	10
1 Introduction.....	12
1.1 Protein- and Gene Therapy	12
1.2 mRNA in the loop.....	13
1.2.1 Gene to Protein	13
1.2.2 mRNA degradation.....	16
1.2.3 Circular RNA	19
1.2.4 Modified mRNA as therapeutic.....	22
1.3 Hypothesis	26
1.3.1 Thesis project aims: Pilot <i>in vivo</i> study.....	26
1.3.2 Proof of principle: Typ I Diabetes Mellitus	27
1.3.3 Reporter mRNA constructs	28
2 Method and Materials	30
2.1 Construction of mRNA templates.....	30
2.1.1 Capped and tailed linear mRNA.....	31
2.1.2 Circular mRNA	32
2.1.3 Outward oriented PCR and sequence verification	32
2.2 <i>In vivo</i> transfection	33
2.2.1 Transfection reagent determination.....	33
2.2.2 TransIT Titration	34
2.2.3 24 hours pilot Flag-detection via Flow Cytometry	34
2.2.4 3-day Time course.....	35
2.3 Protein extraction	35

2.4	RNA extraction and cDNA synthesis	35
2.5	Western blot	36
2.6	Nanoluciferase Assay	37
2.7	qPCR.....	37
2.8	mRNA absolute quantification.....	38
2.9	Hepatocyte isolation with Percoll gradient	38
2.10	Flow Cytometry	38
2.11	<i>In vivo</i> Imaging System (IVIS).....	39
2.11.1	IVIS: 24 hour time point.....	39
2.11.2	IVIS: 4 and 8 hour time points	40
2.11.3	IVIS: Hydrodynamic injection	40
2.12	Statistics.....	40
3	Results	41
3.1	<i>In vitro</i>	41
3.1.1	Gel verification of linear and circular mRNA constructs	41
3.1.2	Circular construct verification with outward oriented PCR/sequencing	42
3.2	Pilot <i>in vivo</i> study	43
3.2.1	TransIT-mRNA revealed as optimal <i>in vivo</i> transfection reagent.....	43
3.2.2	TransIT-mRNA non-toxic range determination.....	45
3.2.3	Flag-tag protein translated in liver from linear and circular mRNA detectable via Flow cytometry 24 hours post-injection	47
3.2.4	Nluc level not detectable through IVIS 24 hours post-mRNA injection of linear or circular mRNA.....	50
3.2.5	Circular mRNA treated mice showed an increased Nluc protein expression between 4 hours and 8 hours post mRNA injection in IVIS whereas linear mRNA derived Nluc level decreased	50
3.2.6	Flow cytometry detected Flag-protein, translated from circular mRNA, suggested to lead to a stronger expression after 24 hours in comparison to linear mRNA derived Flag, however, no difference after three days assessed	54
3.2.7	Circular mRNA levels associated with sustained stability in murine liver in comparison to canonical linear mRNA in 3-day time course experiment	56
3.2.8	Hydrodynamic injection led to higher level of protein expression than standard i.v. injection	57

4 Discussion.....	61
4.1 Linear and circular mRNA constructs	61
4.2 Establishment of <i>in vivo</i> study.....	62
4.3 Ex-vivo 3xFlag-tag detection for linear and circular mRNA treated mice.....	65
4.4 IVIS: Nluc protein biodistribution after standard i.v. injection.....	67
4.5 Circular mRNA associated with beneficial protein and mRNA stability over a time course of 3 days	68
4.6 Hydrodynamic injection led to higher detected Nluc signal.....	69
5 Conclusion	71
List of References	72

List of Tables and Figures

Table 1 Primer sequences for the generation of pilot Nluc and 3xFlag-tag reporter mRNA	30
Table 2 Outward oriented PCR primers	33
Table 3 Primer pair and according sequence for Nluc and Beta Actin qPCR assay	37
Table 4 Mean Fluorescence per cell	49
Figure 1 mRNA degradation pathways	18
Figure 2 In vitro mRNA pharmacology principle.....	24
Figure 3 Hypothesis as overview graphic.....	26
Figure 4 Size difference of linear and circular mRNA	41
Figure 5 Outward oriented PCR for circular construct verification	42
Figure 6 in vivo transfection reagent determination	44
Figure 7 Non-toxic range determination.....	46
Figure 8 Western blot for Flag detection	47
Figure 9 Flow cytometry result after 24 hours of circular and linear mRNA injection.	48
Figure 10 Flow Histogram	49
Figure 11 IVIS 24 hours post-injection	50
Figure 12 IVIS 4 hours and 8 hours post linear or circular mRNA treatment.	51
Figure 13 IVIS 4h and 8h time point experiment.....	52
Figure 14 Absolute copy numbers after 8 hours of circular and linear i.v. injection.....	53

Figure 15 Heat-map of Flag-tag positive cells during a time course of 3 days.....	55
Figure 16 Flag-tag intracellular protein expression in percentage of cell population	56
Figure 17 Absolute mRNA level in murine liver during 3-day time course.	57
Figure 18 IVIS hydrodynamic and standard i.v. injection in comparison.....	58
Figure 19 IVIS hydrodynamic and standard i.v. injection in comparison (cont')....	59
Figure 20 Nluc protein stability of linear and circular mRNA administered via hydrodynamic i.v. injection.....	60

List of Abbreviations

A	Ampere
ATP	Adenosine triphosphate
cDNA	Complementary Deoxyribonucleic acid
CTP	Cytidine triphosphate
DNA	Deoxyribonucleic acid
DNase	Deoxyribonuclease
ELISA	Enzyme-linked immunosorbent Assay
fmol	femtomol
G	Gravitational force
GTP	Guanosine triphosphate
H	Hours
i.p.	Intraperitoneal
i.v.	Intravenous
IVIS	<i>In Vivo</i> Imaging System
IVT	In vitro translation
mM	Milli molar
mRNA	Messenger Ribonucleic acid
N	Number of mice
Nluc	Nanoluciferase
o/n	Over night
PBS	Phosphate buffered saline
qPCR	Quantitative polymerase chain reaction
RLU	Relative Luminescence Unit
RNA	Ribonucleic acid
RNAse	Ribonuclease
Rpm	Rounds per minute
Rpm	Rounds per minute
RT	Room temperature

TBST	Tris buffered saline, 0.1% Tween20
U	Units
UTP	Uridine triphosphate
UTR	Untranslated region
V	Volt
WB	Western blot
μg	Microgram
μl	Microliter

1 Introduction

For organisms and cells it is pivotal to accurately orchestrate a system of several thousand proteins¹. Proteins have diverse roles: catalyze biochemical reactions, provide intra- and extracellular scaffold support, transport molecules or form receptors and channels². Incorrect concentrations and/or mutated proteins are contributing to the rise of medical indications, such as cancer and diabetes^{3,4}. Prominent attempts to address protein aberrations are for instance protein- and gene therapy.

1.1 Protein- and Gene Therapy

Protein therapy is divided into four groups: Group (I): a deficient endogenous protein is replaced by an exogenous protein. Group (II): targeted proteins such as monoclonal antibodies and immunoadhesins. Group (III): prophylactic or therapeutic protein vaccines. Group (IV): recombinant and purified proteins for medical diagnostic use *in vitro* as well as *in vivo*.

The first recombinant protein therapeutic was human insulin belonging to Group (I)². Even though there are many cases in which protein therapeutic was successful, the number of failed, outnumbered nonetheless. Several hurdles are in need to overcome: protein solubility, stability, and route of administration^{5,6}. Furthermore, protein therapy might initiate immuneresponse⁷, post-translational modifications are required⁸, and costs⁹ are issues to be considered.

Another therapy approach to manage diseases involved with protein aberration is gene therapy. By the European Medicine Agency (EMA) gene therapy is defined as a medicinal product with an active substance consisting of recombinant nucleic acid to regulate, repair, replace, add or delete genetic sequences in humans. Furthermore it has to show therapeutic, prophylactic or diagnostic effects¹⁰.

Moreover, gene therapy is classified into two categories: (i) somatic gene therapy, in which nucleic acid is not passed along to the next generation, and the contrary is the case for (ii) germ line gene therapy. However, only the former is allowed for clinical trials with the current legislation¹⁰. Furthermore, in regards to nucleic acid source, further categorization can be applied: ribonucleic acid (RNA) or deoxyribonucleic acid (DNA) as genetic messenger.

In this work we will focus on messenger (m)RNA therapy. The concept of mRNA therapy is to transfer mRNA into the cells and translate the desired pharmacologically active proteins for disease management¹¹. Moreover, mRNA circumvents many caveats DNA gene transfer bears. Unlike DNA, mRNA does not integrate into the genome, and, thus, does not exert the drawback of insertional mutagenesis¹². Further, mRNA is a transient therapeutic for protein replacement, which is in stark contrast to integrative DNA gene transfer¹³. Another advantage of mRNA constructs is its relatively easy engineering, as no nuclear transport, powerful promoter nor terminator are needed. Moreover, mRNA therapy as a cytoplasmic expression system allows transfection of hosts, even with quiescent or slow proliferation – such as muscle cells, brain cell and hepatocytes¹². However, two challenges of mRNA are still faced: immunogenicity and stability^{14,12}, which will be elucidated in chapter 1.2.4 Modified mRNA as therapeutic.

1.2 mRNA in the loop

1.2.1 Gene to Protein

The hereditary information – the genome – of all living cells are stored as double-stranded deoxyribonucleic acid (DNA) inside the nucleus consisting of combinations of four monomer types, the nucleotides¹⁵. DNA was first identified in 1869 by Miescher as “nuclein”, and from then on several scientists contributed to investigate and reveal details about DNA¹⁶. Nucleotides encompass sugar deoxyribose with an attached phosphate group, and a base, either adenine (A),

thymine (T), guanine (G), or cytosine (C). The nucleotides are linked to each other by their sugar through a phosphate group, creating a polymer chain¹⁵.

The DNA is synthesized from a preexisting DNA strand forming complementary structures in which C binds to G, and A to T¹⁵. Further, the two complimentary strands of DNA build a double helix, a structure correctly proposed by Watson and Crick in 1953¹⁷. However, the hydrogen bonds between these base pairs are less strong than the sugar-phosphate bonds, enabling the DNA strands to be separated during the DNA replication process. Then, each strand can serve as a template strand for a new synthesized strand¹⁵.

A key role for DNA is to encode protein sequences. During the transcription process, DNA is converted to ribonucleic acid (RNA). RNA is, similar to DNA, also a linear polymer consisting of repeating monomers. However, RNA is rather single stranded, the sugar is ribose, and uracil (U) is replacing the base thymine (T)¹⁸. Transcription is initiated when the enzyme RNA polymerase binds to the promoter sequence of the template DNA strand upstream – thus 5' end – of the gene. RNA polymerase then catalyzes the synthesis of complementary RNA. The RNA polymerase consists of several subunits, and is typically complexed with other factors when active and attached to DNA. These factors often provide the signal, which gene is to be transcribed¹⁹.

In eukaryotic cells, three types of RNA polymerase exist¹⁹. RNA polymerase I transcribes genes encoding most of the ribosomal RNA (rRNA), RNA polymerase II synthesizes messenger RNA (mRNA) and RNA polymerase III transcribes to yield transfer RNA (tRNA). From these three polymerase types, RNA polymerase II attracted most interest as its mRNA encodes proteins. However, other types of non-coding RNA are also synthesized by this polymerase, such as microRNA and nuclear RNA²⁰.

In eukaryotic cells, enhancer sequences can often be found at a distance upstream of the gene, which it affects. The core promoter for gene transcription by polymerase II is positioned immediately upstream of the gene start site. Furthermore, most polymerase II genes bear a TATA box, which is a consensus sequence of TATTAA affecting transcription rate and defines the location of the

start. As cofactors eukaryotic RNA polymerases utilize several general transcription factors. Due to the looping structure of DNA, enhancers can interact with distal promoters. Proteins facilitating this are termed activators, whilst inhibitors are called repressors¹⁹.

Once transcription had started, strand elongation takes place. Thereby, the DNA double helix unwinds and the RNA polymerase synthesizes according to the template strand, adding the corresponding complementary nucleotides to the 3' end of the generated RNA molecule¹⁹. The approximate rate in eukaryotes is 22-25 nucleotides per second²¹.

Termination of transcription in eukaryotic cells depends on the polymerase molecule. RNA polymerase I stops transcription using a termination factor. RNA polymerase III halts transcription after having transcribed a termination sequence including a stretch containing polyuracil. RNA polymerase II termination process is more complex and needs more research to be fully understood. Transcription of polymerase II genes can surpass the end of noncoding sequence and is cleaved by a complex that associates with the polymerase II. Cleavage appears to be coupled with transcript termination. The resultant mRNA of polymerase II are polyadenylated at their 3'end (poly(A)tail), which is a process with subsequent cleavage and termination of transcription¹⁹.

In prokaryotes, around ten base pairs upstream of transcription initiation site Pribnow box can be found. Moreover, many genes also have an A-T rich upstream element enhancing transcription rate. Once RNA polymerase core enzyme binds, it also associates to another subunit, sigma, to unwind the DNA double helix. This facilitates gene access for transcription. Further, the sigma subunit is promoter specific and thus conveys RNA polymerase where to bind, aiding the turning on and off of genes¹⁹. Prokaryotes have a faster rate of strand elongation (42-54 nucleotides per second) than eukaryotes²¹. Termination is mediated through two types of terminator sequences in close proximity to noncoding sequences: rho dependent and – independent terminators. The former transcribes inverted repeat sequences that fold back to generate a hairpin loop structure. This pauses the RNA polymerase and leads to the release of the transcript. Rho-dependent

terminator utilizes the factor rho, which unwinds the DNA-RNA hybrid generated during transcription, thereby, releasing the synthesized mRNA¹⁹.

For some genes, RNA is the final product, but for most of the genes, mRNA is used as intermediate for protein synthesis. In the translation process, mRNA is decoded into amino acid sequence following the genetic code aided by transfer RNA. Thereby, groups of three consecutive mRNA nucleotides (codon) are translated into one of the common 20 different amino acids or specifies a stop of translation. mRNA has three possible reading frames, depending on where the translation starts. However, only one reading frame encodes the required protein¹⁵.

1.2.2 mRNA degradation

The protein quantity is a function of, not only, its own half-life, but also mRNA synthesis, translation and decay. The abundance of mRNA depends on the efficiency of gene transcription, pre-mRNA splicing, post-transcriptional modifications, and mRNA nuclear export efficiency. Cytoplasmic mRNA degradation can be influenced by similar nuclear processes, altering mRNA metabolism. Degradation of mRNA can be categorized into two classes: elimination of potentially toxic protein production and mechanisms to change mRNA half-life²².

The stability of mRNA is impaired through different degradation pathways. Decay with endonucleases is one pathway, but the major mRNA decay pathway, involving exonucleases, is predominant (**Figure 1**). Exonucleases are enzymes able to degrade on both ends of the nucleic acid molecule²².

mRNAs of eukaryotic cells have at the 5' end of the molecule a 7-methylguanosine cap and at the 3' end a poly(A) tail. They are synthesized co-transcriptionally and contribute to the stability of mRNA as they protect the nucleic acid molecule from exonucleases. Thus, to initiate degradation, these stability determinants need to be compromised, or the mRNA internally attacked by endonucleases.²³

For the exonucleases pathway to begin, the poly(A)-tail is shortened. However, this step is still reversible, as transcripts can encompass signals for readenylation. If these signals are non-existing, the unprotected and susceptible 3' end can then be further attacked through 3' to 5' exonucleases. Moreover, also 5' cap removal can/does take place enabling mRNA degradation in 5' to 3' direction²³.

Endonuclease decay pathway cleaves mRNA producing two fragments which then are prone to exonucleases attacks as well²³.

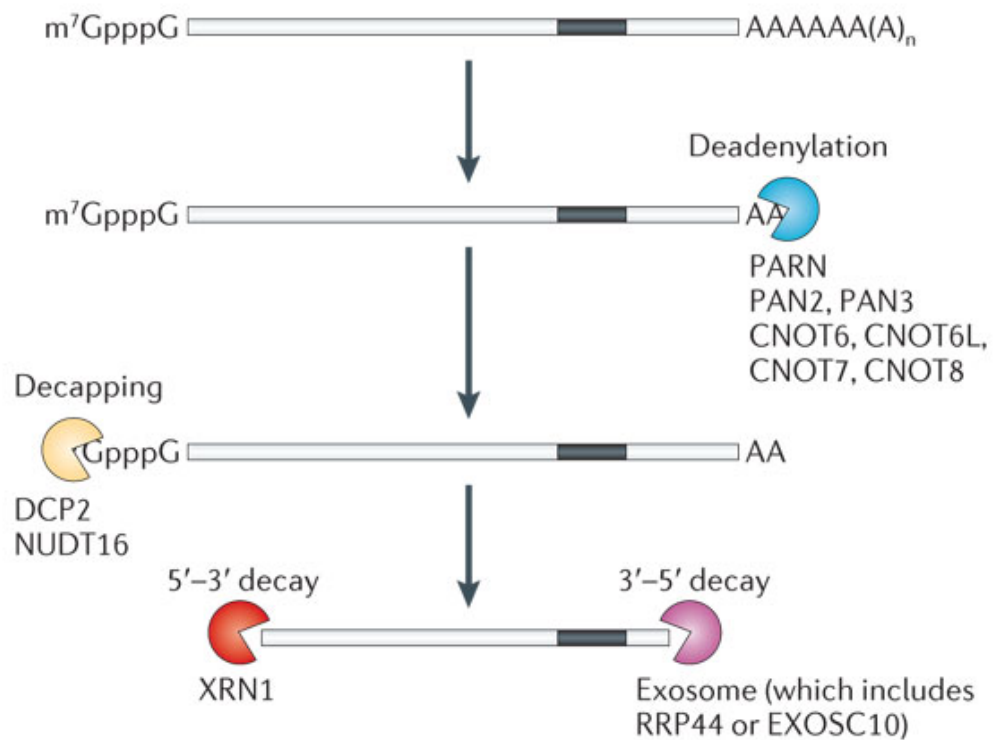
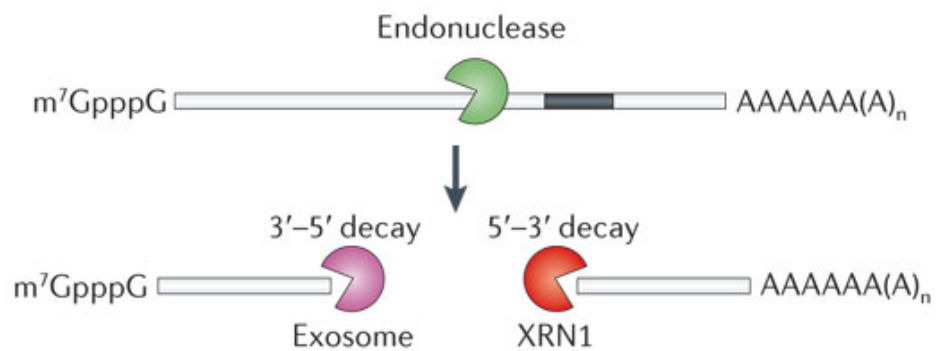
a Exonuclease decay pathways**b Endonuclease decay pathways**Nature Reviews | **Genetics**

Figure 1 mRNA degradation pathways. Major exonucleases pathway starts with shortening of poly(A) tail through deadenylation. Then, the cap is hydrolyzed and the mRNA body gets degraded with 5' to 3' and/or 3' to 5' exonucleases. Other mRNA are degraded internally through endonucleases. Source: Schoenberg and Maquat "Regulation of cytoplasmic mRNA decay"²²

1.2.3 Circular RNA

Interestingly, 1976 naturally occurring circular mRNA were found and first thought to be molecular artifacts of aberrant RNA splicing. Unlike linear RNA, circular mRNA are covalently closed loops. Thereby the 3' and 5' ends, normally present in an RNA molecule, are conjoined. Furthermore, circular mRNA were found to have gene regulatory function (circular mRNA working as sponges to minimize oncogenic microRNA activities²⁴), are abundant, cytoplasmic stable (half-life >48 hours), and presumed to be exonuclease resistant^{25,26,27}.

Recently, through advances in high-throughput sequencing and computer analyses several studies had shown that abundant circular RNA were found throughout species, including in humans. Some circular RNA were found to exist over 10-fold higher than their canonical linear transcript counterpart of the same gene^{28,29}.

Different models of how these circular RNA have arisen are for instance 'exon skipping' and direct "backsplicing". The former describes the idea that the 5' and 3' ends of RNA form a lariat, thereby the 3' end of upstream positioned exon covalently bind to 5' end of a further downstream positioned exon and skipping exons in between. The introns are then removed through splicesome. Direct backsplicing is hypothesized to take place when introns pair through base pairing creating a circular structure. Afterwards, introns are either removed or kept^{28,29}. Other types circular RNAs found are i.e. circular intronic RNA³⁰ and exon-intron circular RNA^{31,29}. However, protein translation from circular RNA have not been found *in vivo* but is debatable³².

In diseases, accumulating evidence imply that circular RNA may be involved in neurological diseases, cancer, atherosclerotic vascular disease, and prion disease and may thus serve as potential biomarkers^{33-35,29}.

Several protocols had been developed to enable *in vitro* circularization of mRNA: splint-mediated³⁶, self-splicing^{37,38}, and enzymatic³⁹. With these techniques the authors stated application perspectives such as structural and engineering studies³⁶⁻³⁹, or for increased stability³⁹.

1.2.3.1 Enzymatic RNA circulation

Beaudry and Perreault described synthesis of circular RNA through enzymatic T4 RNA ligase reaction. The method was subdivided into five steps³⁹:

(i) Mutations and ligation sites were introduced through circularly permuted RNA strategy through PCR-amplification using DNA polymerase. Thus, a transcriptional template was generated for the subsequent cell-free *in vitro* transcription step. To enable run-off transcription, the DNA template had to have a T7 promoter upstream of the coding sequence and needed to end after the stop codon.

(ii) Then, run-off transcription was performed with T7 RNA polymerase. *In vitro* transcription enables to synthesize RNA of any sequence, and as used in this protocol T7 coliphage, a bacteriophage promoter sequence and corresponding RNA polymerase were exploited for transcription of the target. Generally, PCR product, plasmid, or oligonucleotides can be the template for transcription. Naturally occurring transcription terminates at terminator sites, the Rho-independent terminators. Thereby, a hairpin structure (7-20 base pairs) is formed at the 3' end of the mRNA with a subsequent U-rich sequence. The looped secondary structure promotes a halt of the RNA polymerase and thus disrupts the transcription complex. However, in *in vitro* transcription a hairpin structure is not generated and the polymerase "runs off" the end of the template⁴⁰.

(iii) 5' triphosphate of the RNA molecule was substituted by a monophosphate as monophosphate ends can easily get dephosphorylated in contrast to 5' triphosphate. The dephosphorylation step is needed for i.e. 5' end labeling⁴⁰. Moreover, the 5' pyrophosphate removal also triggers mRNA degradation by its 5'-end pathway⁴¹ and, here, can especially be used for subsequent T4 RNA ligation.

(iv) Ligation with T4 RNA ligase was executed to circularize the RNA molecule. T4 RNA ligase is used as a catalyst to form phosphodiester bond between 5' phosphoryl-terminated RNA donor and 3' hydroxyl-terminated RNA acceptor. Thereby, ATP is hydrolysed to AMP and PP_i ⁴².

(v) Transcript analysis on a gel and subsequent purification to yield circular mRNA were performed. In denaturing polyacrylamide gel electrophoresis, circular transcripts have a slower mobility than linear transcripts of the same size. Thus, the two different forms of mRNA can be distinguished from each other accordingly⁴⁰.

1.2.3.2 Self-splicing RNA circulation

The circular RNA is derived from rearranged group I intron through splicing of autocatalytic group I RNA elements^{37,38}.

(i) Plasmid as template should contain self-splicing introns to enable producing circular mRNA.

(ii) In vitro transcription with T7 RNA polymerase with subsequent analysis of RNA product on denaturing polyacrylamide gel.

1.2.3.3 Splint-mediated RNA ligation

Another method to ligate the 5' and 3' ends of RNA molecules is through splint ligation with T4 bacteriophage DNA ligase³⁶. Thereby, the method harnesses the ability of T4 DNA ligase to join RNA molecules when in an RNA:DNA hybrid modification. The DNA oligonucleotide is required to bring the RNA ligation site to proximity to facilitate ligation.

(i) DNA template is required for the subsequent in vitro transcription.

(ii) In vitro transcription from the DNA template with T7 RNA polymerase is performed.

(iii) Using polyacrylamide gel electrophoresis, the *in vitro* transcribed RNA is purified through excising the desired RNA and elution from the gel.

(iv) Next, end labeling and ligation of RNA components was done in this protocol. Thereby, a double-stranded RNA/DNA hybrid is generated with T4 polynucleotide kinase. To successfully ligate, the 3'RNA needs a monophosphate at its 5' end.

(v) The ligated RNA product is then obtained through gel purification.

1.2.4 Modified mRNA as therapeutic

Naturally occurring mRNA (messenger ribonucleic acid) serves as a template deriving from DNA for protein expression. Hence, this intermediate carrier of genetic information can be utilized as means to express proteins of interest through introducing exogenous generated mRNA into target cells⁴³.

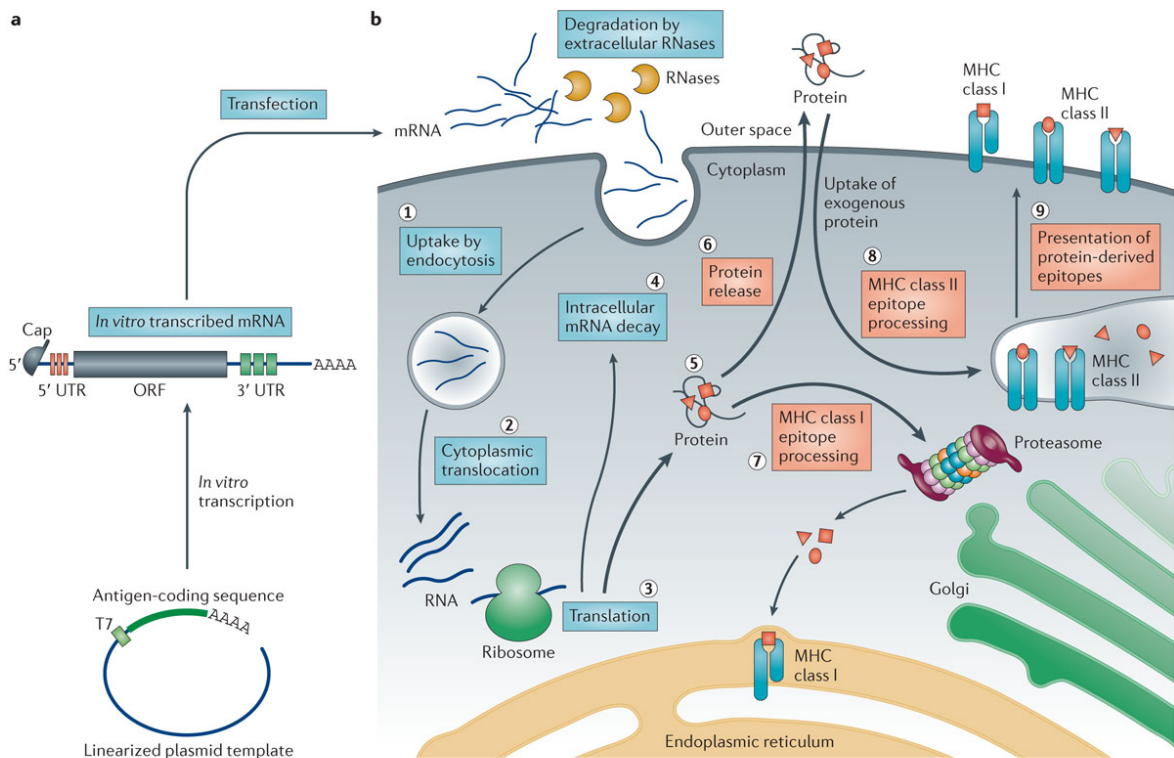
Matured eukaryotic mRNA encompasses five significant features: cap structure at the 5' end of the molecule for i.e. mRNA splicing, stabilization, transport; 5' (5'UTR) and 3' (3'UTR) untranslated region, open reading frame (ORF) and a tail of 100-250 adenosine residues (Poly(A)tails), which is also eminent for efficient translation and stability⁴⁴. mRNA opens a versatile therapeutic avenue for cancer immunotherapies, infectious disease vaccines, allergy tolerization, genome engineering, genetic reprogramming and protein-replacement/supplementation therapies and emerge as a new class of drugs¹¹.

The idea of using nucleic acid as drug began more than two decades ago, when *in vitro* transcribed mRNA or plasmid DNA was injected into skeletal muscle of mice. Through this introduction the encoded protein was expressed⁴⁵. However, mRNA as therapeutic option did not get into focus of attention at that time, due to its instability in comparison to DNA. Thus, methods using plasmid DNA and viral DNA were pursued. Since mRNA discovery in 1961, extensive knowledge about this molecule accumulated, enabling to develop approaches to face the occurring obstacles¹¹.

Conceptually, *in vitro* transcribed mRNA-based therapeutic approaches bears many advantages over DNA-based therapeutics, such as no insertional mutagenesis, and being only transiently active, thus, being a safer strategy. *In vitro* transcribed mRNA-based therapeutic modalities had also entered preclinical and clinical development I.e, in the field of cancer⁴⁶, cardiology⁴⁷, haematology¹⁴, endocrinology⁴⁸.

Two approaches had been used for *in vitro* transcription mRNA therapy: *ex vivo* and *in vivo*. Regarding the former, cells of the patient are isolated, then transfected with mRNA, and returned into the patient. For the *in vivo* approach, mRNA is directly administered and various routes are under investigation¹¹.

Even though eukaryotes can actively engulf naked mRNA, the uptake of mRNA into the cell is hampered by the negatively charged cell membrane. Thus, the transfection rate of cells can be increased through complexing mRNA with agents, facilitating cellular entry and protecting mRNA from degradation⁴⁹. Chemical methods use cationic polymer, cationic lipid, calcium phosphate, cationic amino acid. Through this method, positively charged chemicals complex with the negatively charged nucleic acid. Then, the positively charged chemical/nucleic acid complex are attracted by the opposite charged cell membrane. Through believed endocytosis and phagocytosis the nucleic acid can subsequently enter the cell. The efficiency of transfection depends on factors such as nucleic acid and chemical ratio, and the pH of the solution. Other method of cell entry is through physical means, such as micro injection, electroporation, and hydrodynamic delivery^{50,51}. The principle behind the latter emerging technique is that injecting a high volume (8-10% of murine body weight) within a short time period into the tail vein leads to a hydrodynamic force, permeabilizing the capillary endothelium. Then, the created “pores” in the liver parenchyma cells allow the cytosolic uptake of nucleic acid molecules. Mechanistically, the bolus is directly driven into the inferior vena cava of the liver, inducing a cardiac congestion and the bolus enters the liver in retrograde⁵¹.



Nature Reviews | Drug Discovery

Figure 2 *In vitro* mRNA pharmacology principle. A. Scheme of linearized plasmid used as template for *in vitro* transcribed mRNA. B. Exogenous antigen-encoding mRNA pathway in the cytoplasm. Source: Sahin, Kariko, Türeci “mRNA-based therapeutics—developing a new class of drugs”¹¹

In contrast to endogenous mRNA which enters the cellular cytoplasm after nuclear export, exogenous mRNA enters the cell through the extracellular space. The fraction of *in vitro* transcribed mRNA, which escaped extracellular degradation through ubiquitous RNases, enters the cell (**Figure 2**). In the cytoplasm, mRNA is translated through the host cell protein synthesis machinery. The translated protein can then undergo post-translational modification, act within the cell or is secreted through autocrine, endocrine or paracrine pathways. Protein derived from mRNA encoding antigens for immune-therapeutics are in need to be degraded to obtain antigenic peptides, which then are presented by the major histocompatibility complex (MHC) to immune effector cells¹¹. Termination of translation occurs through physiological metabolic pathway, i.e. major exonuclease decay pathway²².

mRNA therapy bears a great potential and has versatile usage application. However, there are two major limitations – stability and immunogenicity – which are tried to overcome with modifying mRNA¹¹.

Like DNA, RNA can elicit an immune reaction if applied *in vivo* through the mammalian innate immune system, activating the Toll-like receptors (TLRs)⁴⁴. During pathogen infection, TLRs are known to regulate and link the innate and adaptive immune responses⁵². The use of pseudouridine, 5-methylcytidine, 2-thiouridine, 6-methyladenosine, 2'O-methylated and inosine at the 5'-terminal cap had been suggested to reduce immune response⁵³.

To combat mRNA instability, different regions of mRNA can be modified¹¹:

- (i) 5' cap: Use of cap analogues to increase resistance to decapping process.
- (ii) 5' UTR: Incorporate sequences to inhibit 5' exonucleolytic decay.
- (iii) Coding region: Modify bases to reduce endonucleases mediated decay.
- (iv) The whole *in vitro* mRNA: Designing and generation of favourable secondary structures.
- (v) Poly(A) tail: Prolong poly(A) tail or modify nucleotides to escape deadenylation.
- (vi) 3'UTR: Choose sequences that repress mRNA deadenylation.

1.3 Hypothesis

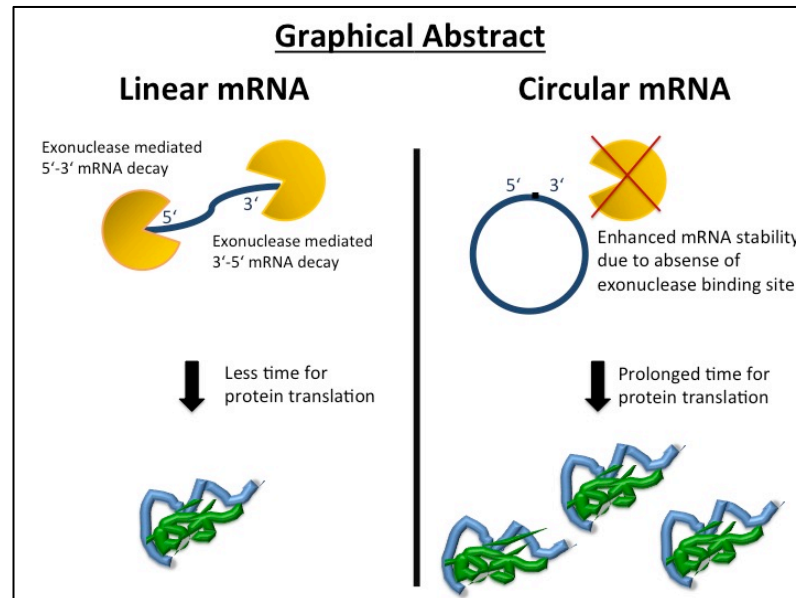


Figure 3 Hypothesis as overview graphic. Through circularizing mRNA, the 5' and 3' binding sites for exonucleases are not accessible. Thus, this enzyme class cannot degrade the nucleotides and, hence, we hypothesize that this circular conformation enables a more stable mRNA template for prolonged protein translation for future therapies.

As mentioned, mRNA-based gene therapy is severely limited by the rapid degradation within the cell²². However, endogenous circular mRNAs have been shown to be stable in cells²⁷. Therefore, the underlying hypothesis of this project is that recombinant circular mRNA, encoding proteins of interest, exhibit enhanced stability *in vivo* in comparison to canonical linear mRNA. Thus, the increased half-life of circular mRNA will prolong protein expression and could have notable use in therapeutic settings (**Figure 3**). This is the first work aiming to use circular mRNA as a possible therapeutic option.

1.3.1 Thesis project aims: Pilot *in vivo* study

The focus of this master project was to characterize the pharmacokinetics of circular mRNA in a pilot *in vivo* study performed in mice.

- Identify safe mRNA delivery into mice

- Determine *ex vivo* and *in vivo* methods to detect reporter nanoluciferase (Nluc) and 3xFlag-tag mRNA and protein expression
- Characterization of pharmacokinetic differences between circular and linear mRNA

1.3.2 Proof of principle: Typ I Diabetes Mellitus

Ultimately, for proof of principle the disease type I Diabetes Mellitus is chosen, as insulin is already FDA approved⁵⁴ and thus would pave the way for circular mRNA therapy to be approved as well, if this concept proves to be functional. Moreover, the preproinsulin is relatively small, facilitating mRNA circularization.

Diabetes poses an emerging public health threat with 422 million adults suffering from diabetes world wide in 2014⁵⁵. This also led the World Health Organization to call for “global action to halt rise in and improve care for people with diabetes” on World Health Day 2016⁵⁶.

This work focuses on type I diabetes (insulin-dependent diabetes mellitus), which is an autoimmune disease. The progression of the autoimmune destruction is mediated by circulating islet autoantibodies targeting beta-cell antigen. Then, self-reactive lymphocyte get activated, infiltrating and destroying the beta-cells. Thus, the underlying basic premise is a deficiency of immunological self-tolerance^{57,58,59}. Beta-cells are situated in the pancreatic islet of Langerhans and are specialized cells producing insulin, the lack of which leads to hyperglycemia. Long-term effects are often neuropathy, retinopathy, and nephropathy^{60,61}. A common and simple treatment regimen is insulin subcutaneous injection to control blood glucose level^{62,63}. The major drawback of this form of treatment is that a good glycemic control usually needs at least three, if not more daily insulin administration⁶³. With enhanced circular mRNA stability and resultant prolongation of protein expression, less insulin injections would be required for diabetes management.

Other interesting therapeutic approaches for type I diabetes are pancreas and islet cell transplantation⁶⁴. To avoid immune response, encapsulated pancreatic islets are under investigation⁶⁰, but also reprogramming liver cells into insulin producing

cells through applying pancreas unique transcription factor⁶⁵. Furthermore, electroporation of bone marrow-derived dendritic cells with mRNA encoding interleukin 4 and subsequent reintroduction into nonobese diabetic mice before or immediately after the onset of hyperglycemia showed promising result of preventing and treating diabetes. However, IL-4 expression was only short-lived, lasting less than 24 hours⁴⁸.

Interestingly, in diabetic mice and rat models proinsulin and insulin producing cells apart from the pancreas were found in liver, adipose tissue, spleen, bone marrow, and thymus. Moreover, non-diabetic mice injected with glucose to simulate hyperglycemia were reported to led to extrapancreatic proinsulin- and insulin-positive cells⁶⁶.

1.3.3 Reporter mRNA constructs

To challenge the hypothesis an mRNA reporter was constructed encoding the proteins nanoluciferase (Nluc) and 3xFlag-tag.

To tag protein epitopes is a powerful methodology for detection as well as purification of proteins. Thereby, the two most widely used epitopes are c-myc and Flag-tags⁶⁷. The Flag-tag is an eight amino-acid short peptide and is hydrophilic⁶⁸. To improve this system, three Flag epitopes in tandem (3xFlag-tag) had been engineered and exhibit superiority in comparison to the single Flag-tag due to increased interaction with the M2 anti-Flag antibodies⁶⁹. We will be using the 3xFlag-tag system to distinguish between endogenous and exogenous insulin in the future time course of this project. In the *in vivo* study shown in this work, the optimal detection method of 3xFlag will be determined as well as used for assessment of any differences between circular and linear mRNA treatment.

To identify the biodistribution of proteins derived from our mRNA reporter construct in mice, Nanoluciferase (Nluc) will be applied. Sensitive detection is enabled when utilizing luciferase enzymes for bioluminescence imaging to investigate cellular and molecular processes *in vivo*⁷⁰. Luciferase are enzymes able to catalyze

reactions which emit light in living organisms⁷¹. This type of technique is not an endpoint analysis and the same mouse can be monitored in respect of its protein biodistribution over a time period. The majority of bioluminescence imaging study until now uses firefly luciferase and other beetle derived luciferases. However, they are comparatively large enzymes (60kDa) and need adenosintriphosphate (ATP) as substrate. These factors however can cause steric problems when fused to the protein of interest and limits the technique to intracellular events, respectively⁷⁰. Hence, accumulating interest lead to search for ATP-independent and smaller luciferases. Thereby, Renilla reniformis (Rluc) is an alternative with a relative small size (34kDa) using coelenterazine as substrate, thus is ATP independent and can be applied for protein secretion and extracellular signaling detection. However, Rluc has low enzymatic turnover and quantum yield^{72,73}. Gaussia luciferase (Gluc) has a molecular weight of 19.9kDa, and thus is three fold smaller than the mentioned beetle luciferase. Furthermore, it also uses coelenterazine as luciferase. However, coelenterazine produces high levels of background luminescence as it oxidizes in serum⁷³. Recently, NanoLuc luciferase (Nluc) derived from the deep-sea shrimp *Oplophorus gracilirostris* had been reported. It has a size of 19kDa and its engineered ATP-independent substrate is furimazine. Nluc has a glow-type luminescence with a half life of over 2 hours with a 150 fold greater specific activity than firefly or Renilla luciferase *in vitro*. Furthermore, with an appending degradation sequence, Nluc is exported from the cell⁷⁴. These features raised interest and studies in mice had been implemented. It had been shown that Nluc can be used for superficial tumors and organs in mice with comparable results as with Gluc⁷⁰. Also in mice, Nluc demonstrated to be a useful tool for systemic metastases and deep brain tumor detection⁷⁵. Nluc also found application in influenza research, thereby allowing real-time infection dynamics⁷⁶.

2 Method and Materials

2.1 Construction of mRNA templates

The protocol was based on the work of Beaudry and Perreault.³⁹ PCR reactions were set up to obtain DNA template with a pUC19 vector encoding Nluc and 3xFlag-tag in its multiple cloning site as follows: The first PCR reaction was performed to integrate 3xFlag into the C-terminal site: Per 1 reaction, 20ng of DNA pUC19 already encoding Nluc was mixed with 1x Q5 Hot Start High-Fidelity Master Mix (New England BioLabs), and forward primer ID Nr-706_F and 707_R for reverse as stated in Table 1 in a total volume of 20 μ l. The PCR condition was set for the initial denaturation at 98°C for 30 second, followed by 35 cycles of 98°C for 10 seconds, 65°C for 20 seconds and 72°C for 30 seconds and a final extension at 72°C for 5 minutes.

Subsequently, a second PCR reaction was executed to add elastin 3'UTR downstream of the inserted 3xFlag-tag. The same procedure as described in the first PCR reaction was followed, except that primers ID Nr-706_F and 708_R were used.

Table 1 Primer sequences for the generation of pilot Nluc and 3xFlag-tag reporter mRNA

Primer ID Nr.	Sequence
706_F	ATCGTA GGTACC TGCCGTCGGTAAAAGAAGGA
707_R	CCCATTACTTGTCGTCATCGTCTTTGTAGTCCTTGTCGTCA TCGTCTTTGTAGTCCTTGTCGTCATCGTCTTTGTAGTCGACG TTGATGCGAGCTGAAG
708_R	TACGATGGATCCTGCCGTCGGTCCCTCCCTCCCTCCCCC ATCCCTCCCTCCCTCCCCCATCCCTCCCTCCCTCCCCCA TACTTGTCGTCATC
566_F	TAATACGACTCACTATAGGGAAAAAAAAAAAAATGCCGTCGG TAAAAGAAGGA
567_R	TTTTTTTTTTTTTTTTGCCGTCGGTCCCTCCCTC

PCR products were then purified using the Quick-Start Protocol PCR Purification Kit (Qiagen) and analyzed on a 1% TAE agarose gel run at 100V for 30 minutes.

To generate the correct DNA template for in vitro transcription (IVT), 20ng/reaction of the obtained PCR product was mixed with 1x Q5 Hot Start Master mix in a total volume of 20 μ l with primer ID 566_F and 567_R run at the conditions described above and purified with QIAquick PCR purification Kit (Quiagen).

For IVT, HiScribe T7 High Yield RNA Synthesis Kit (New England BioLabs) was used with some modification. In short, per reaction 500ng DNA template, 10mM ATP, 10mM GTP, 10mM UTP, 5mM CTP, 5mM 5-methyl cytosine, 40U RNaseOUT Recombinant Ribonuclease Inhibitor (Invitrogen), 2 μ l of T7 Polymerase Buffer, and 2 μ l Polymerase were incubated at 37°C for 2 hours. Subsequently, DNase treatment was performed with 1x DNase I Reaction Buffer and 2U DNase I (RNase Free), both reagents supplied by New England BioLabs. Prior to continuing to generate either capped/tailed or circular mRNA, the RNA was purified via GeneJET RNA Purification Kit (Thermo Scientific) according to the manufacturer's manual.

2.1.1 Capped and tailed linear mRNA

The kit Vaccinia Capping System (New England BioLabs) was used for capping mRNA according to the manual with minor changes as follows: 20 μ g post IVT mRNA product in DEPC-treated water was used per reaction in a volume of 29 μ l and heated up at 65°C for 5 minutes, followed by 5 minutes at 4°C. To the denatured RNA the subsequent reagents were added: 4 μ l 10x Capping Buffer, 1 μ l 10mM GTP, 2 μ l 2mM SAM, 2 μ l Vaccinia Capping Enzyme, and 1 μ l RNaseOUT Recombinant Ribonuclease Inhibitor (Invitrogen). The mix was then incubated at 37°C for 30 minutes and purified (GeneJET RNA Purification Kit, Thermo Scientific) prior to mRNA tailing.

For tailing E. coli Poly(A) Polymerase kit (New England BioLabs) was used according to the manufacturer's handbook including 0.5 μ l RNase OUT and

subsequent incubation at 37°C for 45 minutes as well as purification with Thermo Scientific GeneJET RNA Purification Kit were performed.

2.1.2 Circular mRNA

The mRNA yield of the *in vitro* transcription and purification step (2.1 Construction of mRNA templates) was subjected to RppH treatment (RNA 5'Pyrophosphohydrolase RppH, New England BioLabs). In short, per reaction 10µg of mRNA diluted in water was incubated at 37°C for 1 hour with 1x NEBuffer 2, 20U RppH enzyme, 0.5µl RNase OUT(Invitrogen) in a total volume of 50µl. Afterwards, mRNA was purified with Thermo Scientific GeneJET RNA Purification Kit.

Next, enzymatic circulation was performed applying T4 RNA Ligase I (New England BioLabs). Thereby, per reaction 50µg RNA was incubated for 2 hours at 16°C in a total volume of 200µl with 20µl DMSO, 4µl 20mM ATP, 1x NEBuffer4, 1µl RNase OUT, and 3U T4 RNA Ligase I.

To degrade remaining linear mRNA, 10U RNase R (Epicentre) was added per 5µg mRNA and incubated at 37°C for 1 hour and subsequently purified with Thermo Scientific GeneJET RNA Purification Kit. Constructs were run on 6% Urea gel for 3 hours at 180V, 4°C. For image analyses the software ImageJ was applied.

2.1.3 Outward oriented PCR and sequence verification

From the resultant circular mRNA, cDNA was reverse transcribed using primers 714_cDNA_F and 712_OOPCR_R (Table 2). Outward oriented PCR (OOPCR) with a set-up as described in 2.1 Construction of mRNA templates was performed with 711_OOPCR_F and 712_OOPCR_R (Table 2).

Subsequently, with pMiniT vector (New England BioLab) PCR cloning was performed with the OOPCR products. With the cloned constructs, transformation

into competent e.coli (One Shot TOP10 Competent Cells, Invitrogen) was performed. 1µl ligation reaction was added to 25µl of competent cells and incubated for 30 minutes on ice before subjected to heat shock at 42°C for 45 seconds and returned on ice for another 5 minutes. 500µl of SOC medium was added and incubated at 37°C for 1 hour at 200rpm. 100µl of transformants were then plated onto LB broth plates with 0.1mg/ml Ampicillin over night at 37°C.

For confirmation, a colony was picked, grown over night at 37°C in 2mL of LB broth with 0.1mg/ml Ampicillin, mini prepped (Qiagen), and sequenced (GeneWiz) using primer 714_M13F and 712_OOPCR_R (Table 2).

Table 2 Outward oriented PCR primers

Primer ID	Sequence
714_cDNA_F	GTAACCATCAACGGAGTGAC
711_OOPCR_F	CTCACGGCTTTCCGCCTGAG
712_OOPCR_R	GTCCCAACGAAATCTTCGA
715_M13_F	GTAAAACGACGGCCAGT

2.2 *In vivo* transfection

Female Balb/c mice, aged 9-12 weeks were obtained from the Jackson Laboratories (Maine), group housed and maintained in a controlled Institutional Animal Care and Use Committee (IACUC) accredited environment at the Dana-Farber Cancer Institute Animal Facility with water and food *ad libitum*. The animals were assigned randomly to the groups; all experiments were reviewed and approved by IACUC and performed following the animal facility guidelines.

2.2.1 Transfection reagent determination

For *in vivo* transfection the following reagents were used per mouse according to the manufacturer's manual: Invivofectamin 3.0 (Invitrogen), *in vivo* TurboFect (Thermo Scientific), Lipofectamine RNAiMAX (Invitrogen), and TransIT-mRNA

(Mirus). As control, mRNA was diluted in PBS. For all tail vein injection a volume of 100 μ l was used, except for InvivoFectamin 3.0 where 200 μ l was applied. Total amount of 20 μ g mRNA per mouse was injected into the mice' lateral tail vein with a 29 gauge needle (BD 0.3ml U-100 Insulin Syringes). 24 hours after treatment mice were sacrificed in a CO₂ chamber according to IACUC guidelines. The liver was dissected and washed in ice cold PBS. Subsequently, approximately 50mg liver was subjected to RNAlater (Ambion) for short time storage until RNA extraction (see 2.4 RNA extraction and cDNA synthesis) was performed. Another 50mg liver tissue was placed into 500 μ l RIPA Buffer (Sigma-Aldrich) for immediate protein isolation (see 2.3 Protein extraction). Nluc Assay (see 2.6 Nanoluciferase Assay) as well as qPCR (see 2.7 qPCR) were performed. The experiment was performed in duplicates.

2.2.2 TransIT Titration

Total volume of 8, 14 and 21 μ l of TransIT-mRNA mixture were injected in 200 μ l total volume per mouse *i.v.* into each mice tail vein. As controls RNAiMax as well as no transfection reagent were used. After 24 hours mice were sacrificed and downstream analyses were performed as described in 2.2.1 Transfection reagent determination.

2.2.3 24 hours pilot Flag-detection via Flow Cytometry

Two mice were *i.v.* injected with 20 μ g of linear or circular mRNA with 10 μ l TransIT transfection reagent in a total injection volume of 100 μ l. As control, Opti-Mem (Gibco) without mRNA was injected to a third mouse. After 24 hours the mice were sacrificed, liver isolated *and* 2.9 Hepatocyte isolation with Percoll gradient with subsequent analyses on a flow cytometer according to were performed.

2.2.4 3-day Time course

20µg/100µl linear (n=3) or circular (n=3) mRNA were injected *i.v.* into each mouse (including 7µl TransIT-mRNA). As control one mouse was injected with media Opti-MEM (Gibco) only. After 24, 48, and 72 hours one mouse of each group was sacrificed. The liver was dissected, analyzed via flow cytometry (2.10 Flow Cytometry without Percoll gradient step) for protein expression and via qPCR for absolute mRNA quantification (2.4 RNA extraction and cDNA synthesis/mRNA absolute quantification).

2.3 Protein extraction

With a hand homogenizer (Pellet Pestle - Kimble Kontes) the liver tissue was homogenized in RIPA buffer and incubated on ice for 30 minutes. Afterwards the samples were centrifuged at 10,000g for 20 minutes at 4°C. The protein concentration in the supernatant was determined through performing bicinchoninic acid assay (Pierce BCA Protein Assay Kit).

2.4 RNA extraction and cDNA synthesis

Liver tissue was placed in 1ml TRIzol Reagent (Invitrogen) and homogenized with a hand homogenizer. The lysate was then incubated for 5 minutes at room temperature. 200µl chloroform was added, followed by shaking the samples vigorously for 15 seconds and incubated for another 3 minutes. Next, the samples were centrifuged at 12,000g for 15 minutes at 4°C. 500µl of the colorless upper phase is mixed with an equal volume of 70% Ethanol and mixed thoroughly. PurLink RNA Mini Kit was used to continue total RNA isolation.

For cDNA synthesis 500ng mRNA/reaction was used using Random Hexamers (Invitrogen) and Superscript IV Reverse Transcriptase (Invitrogen) according to the manufacturer's manual with small modification as follows: after all the reagents

had been added, the samples were incubated at 23°C for 10 minutes, 42 °C for 50 minutes, 80 °C for 10 minutes and 4°C for 1 minute after which 5U of Rnase H is added per reaction and incubated for another 37°C for 20 minutes and stored at -20°C until used.

2.5 Western blot

The murine liver lysate obtained after step 2.3 Protein extraction was assessed with western blot through a combination of protocols^{77,78,79} with some modifications: As size marker Page Ruler Prestained Protein Ladder (Thermo Scientific, IL USA) was used. 20µg, 40µg or 125µg protein per sample was heated at 85°C for 2 minutes, then subjected to each well of a 16% Tricine gel for separation using 30V for 1 hour, followed by 100V for 3 hours and 300V for 1 hour at 4°C. As control, Carboxy terminal Flag-Bap Fusion Protein (Sigma) was used. Wet transfer onto a polyvinylfluoride membrane (GE Healthcare) was performed through electrophoresis applying 0.2A for 1 hour at 4°C. Next, the PVDF membrane was blocked with 3% milk in TBST o/n at 4°C and washed three times for 5 minutes each with TBST. Subsequently, the membrane was incubated with anti-Flag M2 monoclonal antibody (1:1000, Sigma Aldrich F1804), Monoclonal Anti Flag M2 Peroxidase Clone M2 (1:1000, Sigma Aldrich) or Beta-Actin Primary Antibody (1:5000, Sigma Aldrich), DYKDDDDK Tag (1:1000, Cell Signaling), Nluc (1:1000, Promega) for two hours at room temperature. After washing the membrane three times TBST for 5 minutes, the membrane was then incubated with 1:20,000 anti-mouse antibody (Abcam, Goat F(ab) polyclonal Secondary Antibody to Mouse IgG - H&L (HRP)) at room temperature for 1 hour. After another wash as prior described, the membrane was treated with ECL reagent (Amersham ECL Prime Western Blotting Reagent) before exposed to x-ray film (KODAK Carestream Medical X-ray Film General Purpose Blue) for development.

2.6 Nanoluciferase Assay

In triplicates 50µg or 100µg murine protein liver lysate were analyzed with Nano-Glo luciferase Assay System (Promega) as described by the manufacturer's manual except that Nano-Glo Luciferase Assay Substrate was mixed with Glo Lysis Buffer (Promega).

2.7 qPCR

cDNA corresponding to 500ng murine liver RNA (2.4 RNA extraction and cDNA synthesis) was diluted 1:6 and 5µl was analyzed per reaction in triplicates. Power SYBR Green PCR Mastermix (Applied Biosystems) was used with Nluc or Beta-Actin primers noted in Table 3 Primer pair and according sequence. qPCR (Gene Amp PCR System 9700 Applied Biosystems) setting was 95°C for 10 minutes, 40 cycles of 95°C for 15 seconds and 60°C for 1 minute. The relative levels were calculated in respect to the expression levels of Beta Actin and to the median expression of the sample named in the respective experimental result section. The error bars in the graphs indicate standard deviation of triplicates.

Table 3 Primer pair and according sequence for Nluc and Beta Actin qPCR assay

Primer	Sequence
Beta Actin Forward	GACGAGGCCAGAGCAAGAGAGG
Beta Actin Reverse	GGTGTGAAGGTCTCAAACATG
Nluc Forward (683)	TTTCAGAATCTCGGGGTGTC
Nluc Reverse (684)	ACCAGTGTGCCATAGTGACG

Primer assay efficiency for Nluc (109.9%) and Beta-Actin (97.4%) was calculated through generating a standard curve with cDNA diluted 1: 5 as starting point followed by four consecutively 1:2 dilution steps.

2.8 mRNA absolute quantification

A standard curve of Nluc-flag tagged plasmid molecule was created with 30, 300, 3000, 30 000 and 300 000 copies⁸⁰. qPCR was performed as described in 2.7 qPCR, Equal amount of cDNA (250ng) were used to determine mRNA absolute copy numbers through calculation from the standard curve derived equation.

2.9 Hepatocyte isolation with Percoll gradient

To isolate murine hepatocyte, liver was dissected from mice, washed in cold calcium free PBS, minced and passed through a 70µm cell strainer and washed three times with PBS and centrifuged at 12,000rpm for 5 minutes. The pellet is resuspended in Collagenease/Dispase (Sigma-Aldrich) in RPMI and digested at 37°C for 30 minutes. The digestion is stopped by adding 20ml PBS and centrifuging 12, 000 rpm for 5 minutes. The supernatant was then discarded and the pellet washed twice with PBS. Next, the pellet was resuspended in 6ml PBS. The liver homogenate was then resuspended in 5ml PBS. 1.5ml of 1.12g/ml Percoll solution is laid at the bottom of a 15ml tube, followed by 2.5ml of 1.08g/ml and 2.5ml of 1.06g/ml Percoll solution. On top 6ml liver cell suspension is pipetted on top of the gradient. The sample is fractionated by centrifugation at 750g, 20 minutes without break at 20°C. Afterwards the distinct red band was collected and resuspended in 5ml PBS with 5% FBS and subsequently were stained for flow cytometry.

2.10 Flow Cytometry

For flow cytometric analysis, 2×10^6 cells were pre-treated with anti-mouse CD16/21 (Biolegend) 1:200 in PBS with 2%FBS for 20 minutes on ice (to decrease non-specific Fc receptor binding), then washed 3 times with PBS and centrifuged for 10 minutes, 400g at 4°C. To measure viability cells were incubated with

Zombie Aqua (Biolegend) 1:500 in PBS with 2%FBS for 20 minutes in the dark on ice. After 3 PBS washes the cells were fixed with 100µl Fixation Buffer (eBioscience) and incubated in the dark at room temperature for 30 minutes. Samples were then washed twice with 600µl Permeabilization buffer (eBioscience), centrifuged for 5 minutes at 500g at 4°C. Afterwards the pellet is resuspended in 200µl of permeabilization buffer and incubated with the respective antibody according to the manufacturer, if not otherwise stated. Monoclonal anti Flag M2-FITC (Sigma-Aldrich) 1:200, Alexa Fluor 700 anti mouse Ki67 (Biolegend), IgG1-FITC Isotype Control (Sigma-Aldrich), PE Hamster Anti Mouse CD95 (BD Biosciences) and incubated at 4°C for 45 minutes in the dark. The cells were then washed and resuspended in 400µl PBS with 2%FBS. Per sample 10,000 events were acquired with the flow cytometer (BD LSR Fortessa X-20) and assessed with the software FlowJo 10.1r5 (FlowJo Enterprise).

2.11 *In vivo* Imaging System (IVIS)

For all IVIS experiments the following procedure was performed for visualization: Per mouse 20µg Furimazine (Promega) in 200µl PBS was injected *i.p.* 5 minutes prior *in vivo* imaging (Xenogen Imaging) at a ventral position, medium binning, and 1 f/stop. Data were analyzed via Living Image 4.2 Software (Caliper Life Sciences).

2.11.1 IVIS: 24 hour time point

Female BALB/c mice were *i.v* injected with 30µg/150µl of circular (n=2) or linear (n=2) mRNA (including 10.5µl TransIT-mRNA). As control Opti-MEM media (Gibco) without mRNA was injected 24 hours post injection mice were imaged via IVIS.

2.11.2 IVIS: 4 and 8 hour time points

Three female BALB/c mice were allocated into each circular or linear mRNA treated group and received 20µg, 40µg or 80µg mRNA/200µl injection (including 14µl TransIT-mRNA). As control Opti-MEM media without mRNA was used. After 4 and 8 hours post injection, mice were imaged via IVIS. Furthermore, after 8 hours mice were sacrificed and liver dissected and analyzed for absolute mRNA quantities (2.4 RNA extraction and cDNA synthesis; 2.8 mRNA absolute quantification).

2.11.3 IVIS: Hydrodynamic injection

Three female BALB/c mice were subjected for each group, treated either with linear or circular mRNA. For naked mRNA hydrodynamic i.v. injection in mice, 20µg linear or circular mRNA in a volume of 1ml PBS was injected. For hydrodynamic injection with transfection reagent, 20µg linear or circular mRNA was complexed with 14µl TransIT-mRNA reagent and PBS adjusted to a volume of 1ml to be injected per mouse. Standard i.v. injection was performed as described before with 20µg linear or circular mRNA injected with 14µl TransIT-mRNA reagent adjusted with PBS to a total volume of 200µl per mouse. As control, PBS alone was injected per standard i.v.. Time points of in vivo imaging was 4, 8, 24, and 72 hours post-injection. Afterwards, liver was isolated and Nluc protein level was measured as described prior.

2.12 Statistics

Statistical analyses were performed using GraphPad Prism software version 5.02 (GraphPad Software, Inc).

3 Results

3.1 In vitro

The following will briefly focus on the verification of circular mRNA, which will be used in the *in vivo* study. The generated reporter mRNA encodes nanoluciferase (Nluc) and 3xFlag-tag.

3.1.1 Gel verification of linear and circular mRNA constructs

To visualize mRNA, linear and circular mRNA were run on a 6% urea gel for 3 hours at 180V. Linear mRNA led to one band, whilst after circularization step, two bands were visible for circular mRNA sample (**Figure 4**). Due to the conformation, circular mRNA migrates slower than same length linear RNA.²⁷ Thus, the upper band is circularized mRNA. However, a strong band at the same size as linear mRNA was visible as well. Using image analysis, 33% of the circular mRNA sample was determined to be running at slower pace and, thus, is defined as circular mRNA. With exonuclease RnaseR treatment, remaining linear mRNA was degraded.

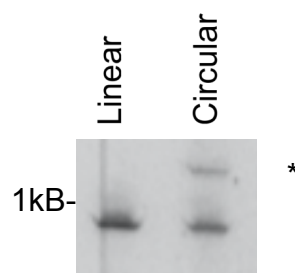


Figure 4 Size difference of linear and circular mRNA. Lower band resembles linear mRNA, upper band shows circularized mRNA, indicated with an asterix.

3.1.2 Circular construct verification with outward oriented PCR/sequencing

Successful circularization of mRNA was further verified via outward oriented PCR and sequencing. While canonical linear mRNA has 5' and 3' ends, circular mRNA lacks these features. Thus, primers (indicated red in **Figure 5, A**) can be positioned to yield only in a product, when the ends of the molecule are indeed conjoined. **Figure 5, B** indicates the successful sequence verification of circular mRNA – with the 5'–3' junction highlighted in red.

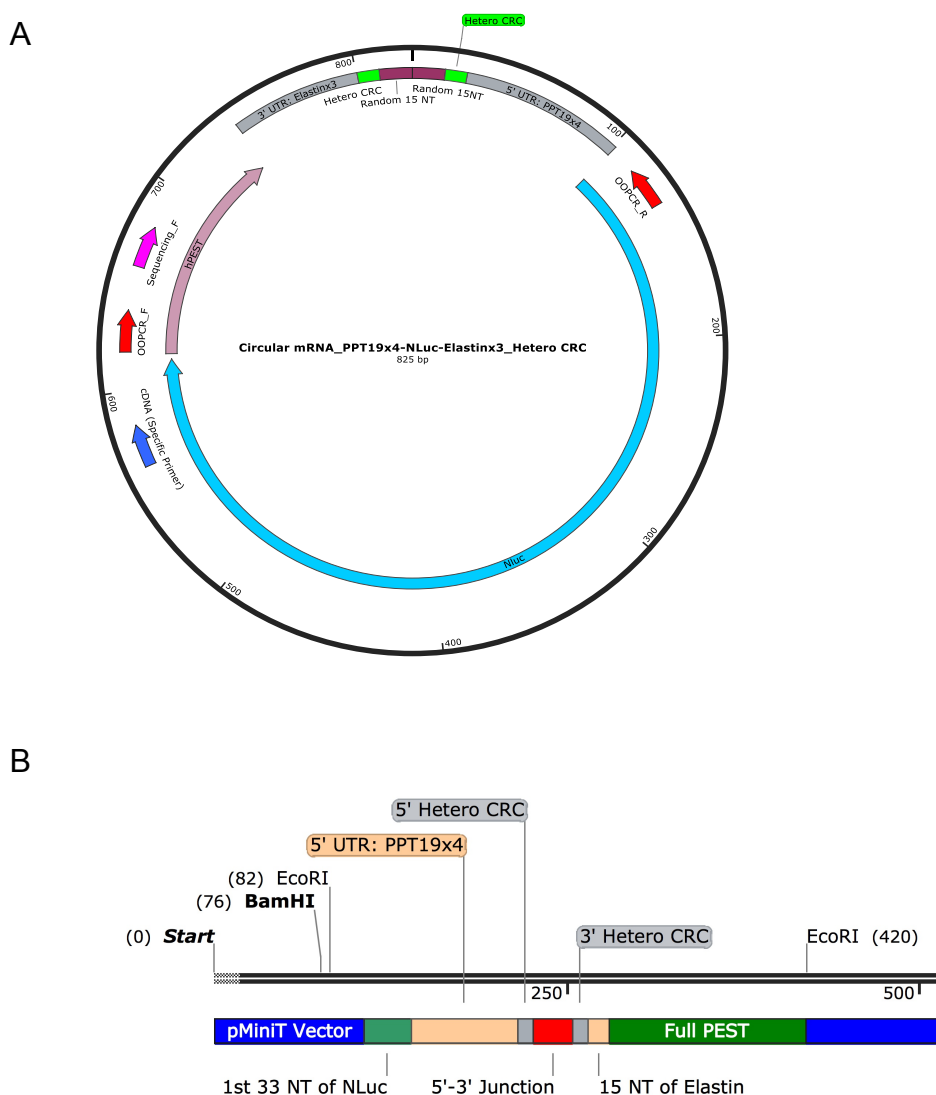


Figure 5 Outward oriented PCR for circular construct verification. (A) Schematic representation of experimental set-up. Red arrows represent forward and reverse primers. (B) Sequencing result visualized with focus on junction site. Only circular constructs can yield in the obtained 5'-3' junction sequence indicated in red.

3.2 Pilot *in vivo* study

These pilot *in vivo* studies were performed to obtain a first insight in how circular and linear mRNA reporter construct, encoding Flag-tag and Nanoluciferase (NLuc), perform in mice when injected through intravenous injection *via* the lateral tail vein.

3.2.1 TransIT-mRNA revealed as optimal *in vivo* transfection reagent

In order to transfect murine liver with mRNA, we use *i.v.* injections into the tail vein of female BALB/C mice. One of four different commercially available transfection reagents (InvivoFectamin 3.0, Turbofect, RNAiMAX, TransIT-mRNA) were injected into mice. As controls, mice were injected with mRNA in PBS (“No carrier”) or were not injected at all (“Untransfected”) (**Figure 6**). Experiments were performed in duplicates in female Balb/c mice. 24h hours post injection, mice were sacrificed in a CO₂ chamber, and their livers analyzed to evaluate their Nluc mRNA (**Figure 6, A**) and protein level (**Figure 6, B**). The relative levels were calculated in respect to the untransfected control. qPCR and NLuc assay of the target tissue demonstrated TransIT-mRNA as the optimal transfection reagent in regards to highest mRNA level and protein expression of the introduced mRNA encoding the reporter Nluc. The pilot experiment showed that Nluc mRNA transfected with TransIT-mRNA lead to a 3×10^5 fold increase of mRNA level in comparison to the untransfected control. Untransfected and no carrier control did not differ in Nluc relative mRNA level. For protein level in liver lysate, Nluc assay was applied to quantify the Nluc protein expression. Thereby, highest level of relative luminescence value was obtained through transfection with TransIT-mRNA (161RLU), whereas the other transfection reagents yielded in RLU values below 50RLU. However, of the two mice injected with TransIT-mRNA, one died immediately after *i.v.* injection and the second reacted lethargic for several minutes after treatment. Therefore, while TransIT-mRNA at this dosage (28 μ l) exerted the most efficient mRNA delivery into mouse liver, it also had a toxic or lethal effect on mice.

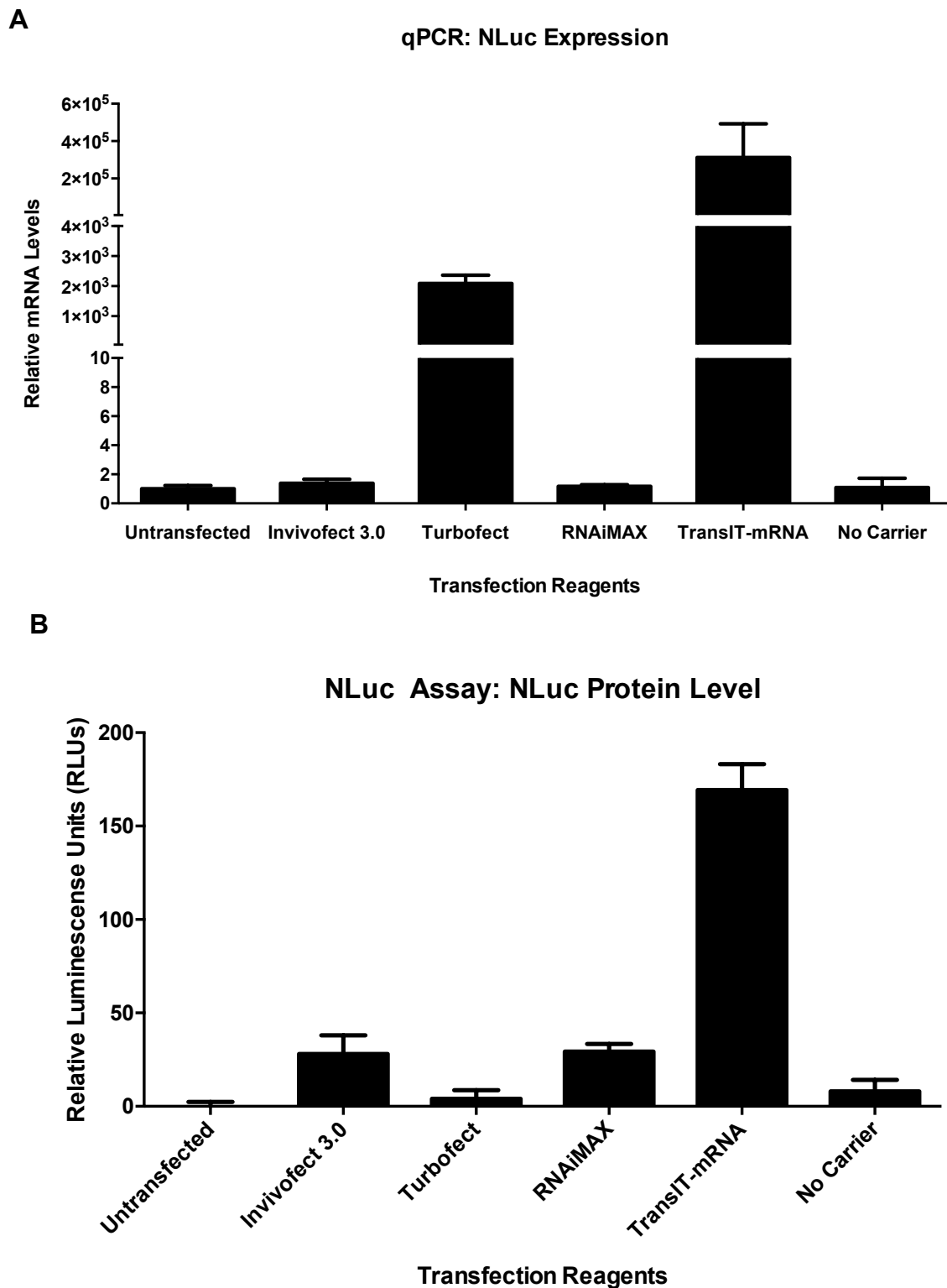


Figure 6 *in vivo* transfection reagent determination. The graphs show the results of analyzing the reporter NLuc in murine liver via (A) qPCR and (B) NLuc Assay. The analyses demonstrated that TransIT lead to the highest NLuc mRNA and protein level, respectively. Error bars indicate standard deviation of triplicate.

3.2.2 TransIT-mRNA non-toxic range determination

As toxicity was observed with the previously used volume of TransIT-mRNA injected into mice (28.6 μ l), titration experiments were performed with different volumes of TransIT-mRNA. Linear mRNA load of 20 μ g was remained constant as well as the 2:1 ratio of the TransIT-mRNA reagent:boost volume. In **Figure 7** all applied transfection reagent volume and the resultant relative Nluc mRNA level in comparison to liver of RNAiMAX transfected mice (**Figure 7, A**) and Nluc protein relative luminescence (**Figure 7, B**). With 21 μ l TransIT-mRNA, the mice started to exhibit slight signs of toxicity, notably mice briefly exhibited breathing problems following tail vein injection, but recovered shortly after. From this observation it was concluded that the best dosage tolerated as well as not producing life-threatening toxicity after injection had to be below 21 μ l TransIT-mRNA. Using 14 μ l TransIT-mRNA, the Nluc mRNA level determined by qPCR and Nluc protein level assessed through Nluc assay showed acceptable signal levels. Moreover, a direct proportional relationship can be observed between the volume of TransIT-mRNA injected and Nluc mRNA level detected in murine liver. However, for protein Nluc expression, a peak in effective transfection was reached at 21 μ l, as using 28 μ l TransIT-mRNA the Nluc protein level decreased by 100RLU. Thus, exerting a similar level as seen with 14 μ l TransIT-mRNA administration.

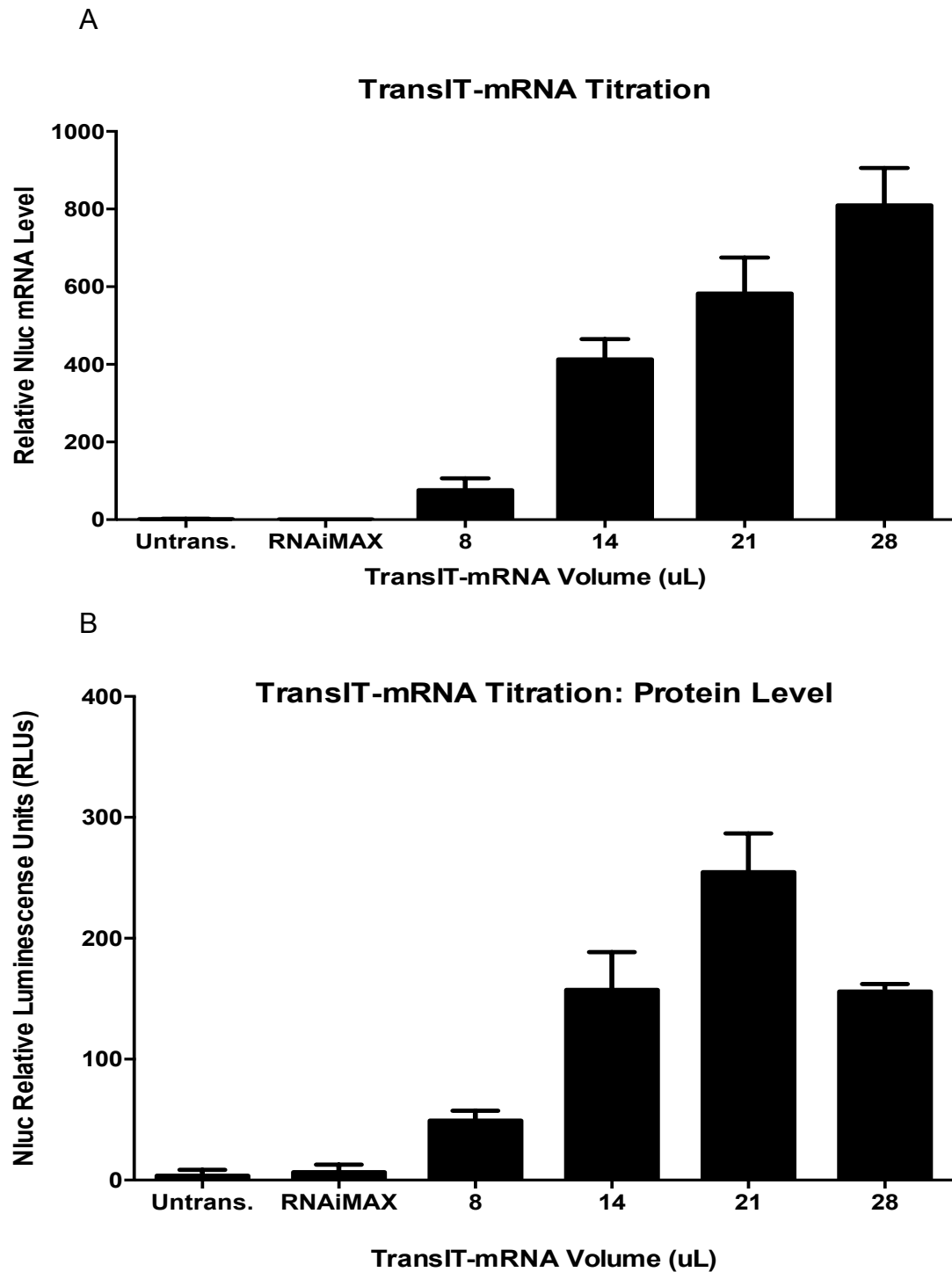


Figure 7 Non-toxic range determination. Different volumes of TransIT-mRNA with linear mRNA were injected into mice to determine the non-toxic range. Further, also (A) mRNA and (B) protein level of Nluc were assessed. Error bars indicate standard deviation of triplicate.

3.2.3 Flag-tag protein translated in liver from linear and circular mRNA detectable via Flow cytometry 24 hours post-injection

For future investigation of circular mRNA as promising therapeutic contender, the mRNA construct will be encoding mouse preproinsulin and a 3xFlag-tag. Hence, the Flag-tag detection is of eminent importance to distinguish between exogenous and endogenous insulin. We approached several protein detection methods such as Western blotting (**Figure 8**) and ELISA. Per mouse, a different set of transfection reagents were used and 20 μ g of linear mRNA were injected *i.v.*. 24 hours later the mice livers were dissected, whole protein concentration of the homogenized liver was determined via BCA assay and 20 μ g and 40 μ g of proteins were analyzed. Only the commercially available positive Flag-tag control gave a signal, but none of the liver lysate samples. Different antibodies against Flag or Nluc were then tested, but did not give any signals. Likewise, ELISA, with and without prior Flag-immunoprecipitation for Flag-tag enrichment gave negative results as well (Data not shown).

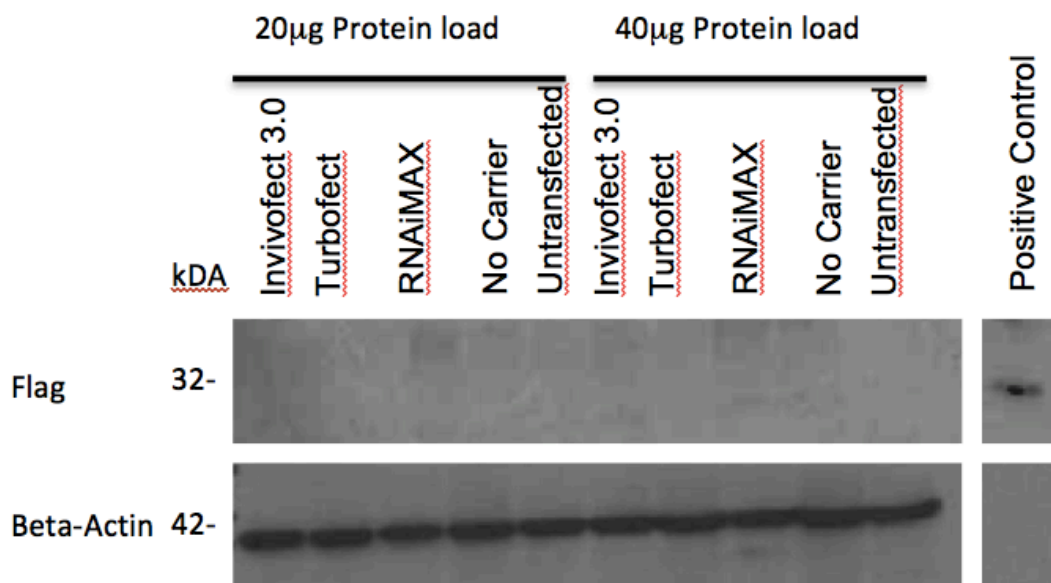


Figure 8 Western blot for Flag detection. Except for the commercially available Flag positive control, none of the analyzed liver lysate showed a positive signal. Beta-Actin was used to show equal protein load.

We next used flow cytometry to assess 3xFlag-tag protein expression in cells. Linear and circular mRNA were administered *i.v.* into mice. As controls, mice were injected with media without mRNA (“No mRNA Control”). A Percoll gradient was used to enrich hepatocytes⁸¹, then the cells were stained with antibodies to enable fluorescence detection of Flag-protein and the viability of cells with flow cytometry. Circular mRNA lead to 41.7% of hepatocytes expressing the Flag protein, whereas 59.5% of liver cells gave a positive Flag signal after linear mRNA treatment (Figure 9).

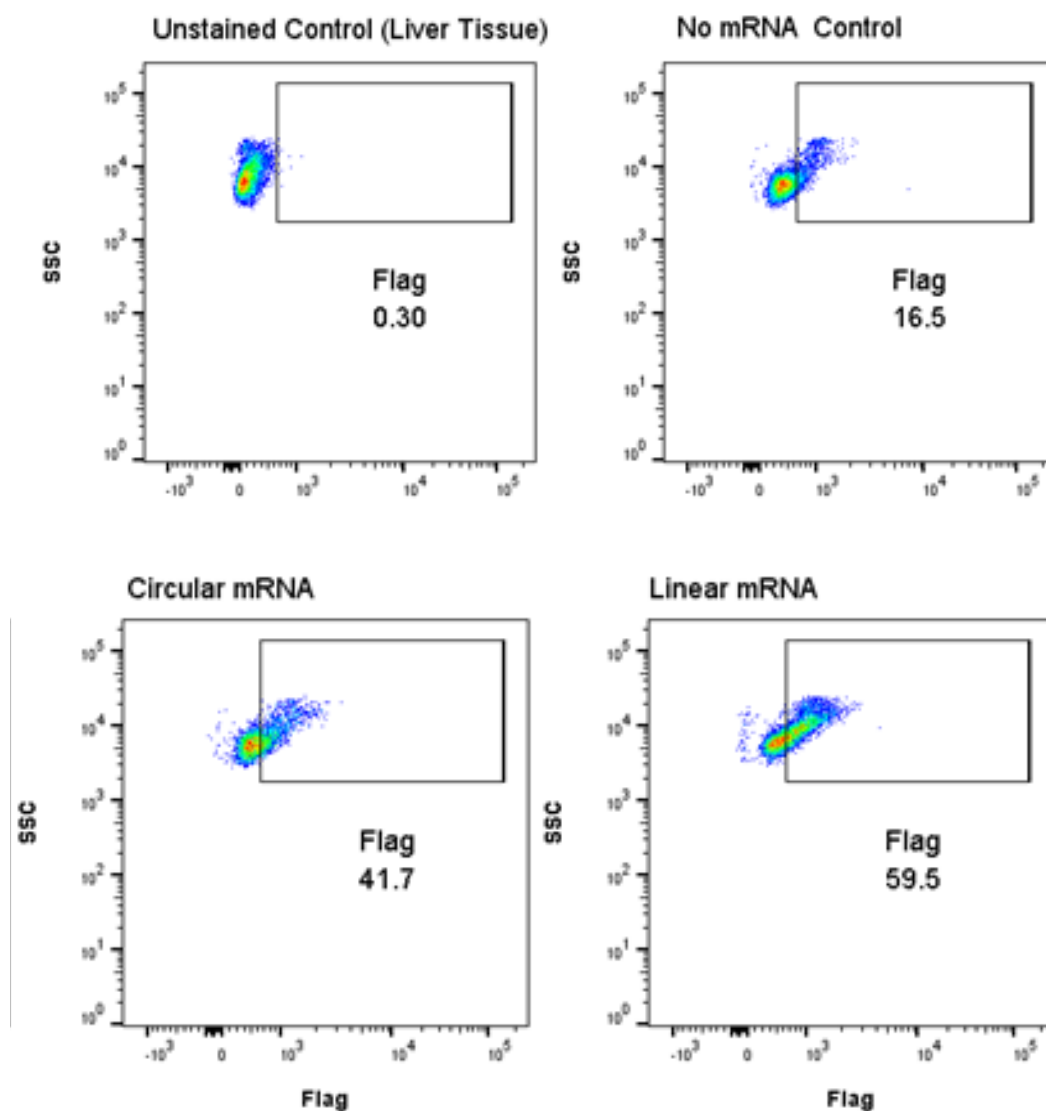


Figure 9 Flow cytometry result after 24 hours of circular and linear mRNA injection. Linear mRNA lead to 20% higher Flag-tag positive cell population than circular mRNA treated cells. No mRNA Control also stained with Flag-FITC antibody emitted 17% of unspecific background.

The results obtained from this experiment were also analyzed through using the mode to graph which relative fluorescence intensity most percentage of cells (in respect to its gated population) were emitting (**Figure 10**). The shift in peak to a higher relative fluorescence value designate, that the majority of cells express higher amount of intracellular Flag-tag. Thus, linear mRNA derived Flag-tag (red) had most cells expressing highest amount of Flag-tag, followed by circular mRNA transfected cells (blue), no mRNA control (orange), and linear unstained control (grey).

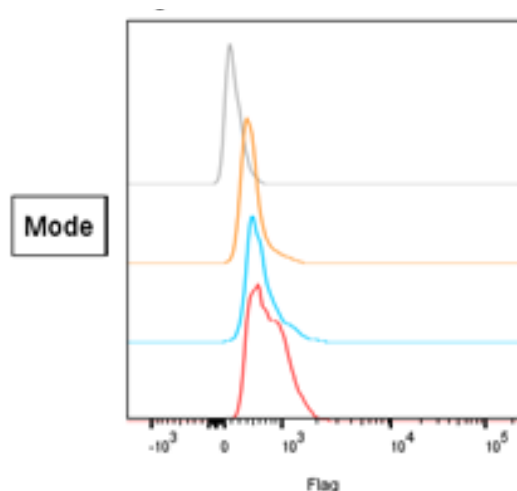


Figure 10 Flow Histogram. Peak shows the relative fluorescence intensity, which most cells – given as percentage of all cells in the population of interest – emit. (*i.v.* treatment: red=linear mRNA, blue=circular mRNA, orange=no mRNA control, grey=linear mRNA unstained control).

The result of investigating the most frequent fluorescence intensity value emitted by individual cells, and thus mirroring amount of flag-tag proteins per cell, is shown in Table 4. Thereby, hepatic cells transfected *in vivo* with linear mRNA has the highest Flag-tag protein expression per cell.

Table 4 Mean Fluorescence per cell

Sample	Geometric mean: Flag-FITC-A
Linear unstained control	229
No mRNA control	490
Circular mRNA	639
Linear mRNA	744

3.2.4 Nluc level not detectable through IVIS 24 hours post-mRNA injection of linear or circular mRNA

The previous experiment showed that Flag-protein of our reporter construct was expressed 24 hours post injection. As the construct also encodes Nluc, we aimed to observe the *in vivo* distribution of translated protein from our mRNA constructs by IVIS. Therefore, mice were subjected to the live imaging apparatus 24 hours after injection with either linear or circular reporter mRNA construct, encoding the 3xFlag-tag as well as Nluc protein. The substrate Furimazine was injected *i.p.* 5 minutes prior IVIS assessment, generating luminescence when it reacts with Nluc protein⁷⁴. No luminescence and, therefore no Nluc, was detectable 24 hour post administration of circular nor linear mRNA (**Figure 11**).

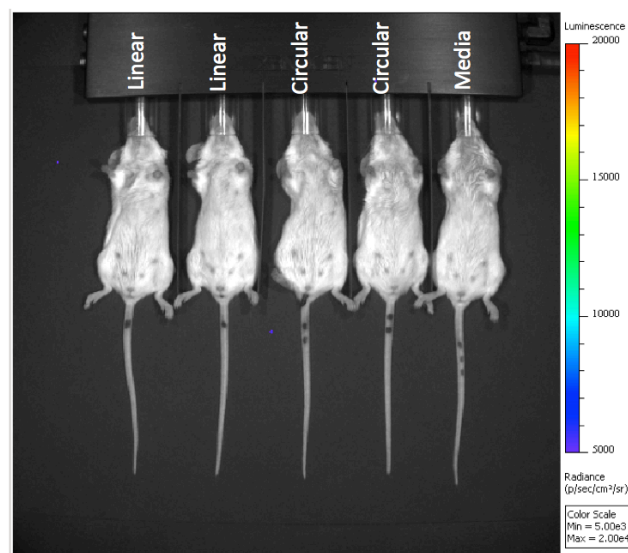


Figure 11 IVIS 24 hours post-injection. No signal detectable in linear as well as in circular treated mice.

3.2.5 Circular mRNA treated mice showed an increased Nluc protein expression between 4 hours and 8 hours post mRNA injection in IVIS whereas linear mRNA derived Nluc level decreased

As protein could not be detected 24 hour post-injection, shorter time points were chosen. Specifically 4 and 8 hours, as it has been previously reported⁸². In

Figure 12 linear mRNA transfected mice showed strong signal at the location of the right peritoneum at dosage 20 μ g and 40 μ g using 14 μ l Trans-IT reagent in the injection volume. After 8 hours post injection of these dosages the signal, and thus the Nluc protein, transitioned toward the mice' mid section but emitted a lower signal. Furthermore, at the same time point 80 μ g of linear mRNA also lead to Nluc expression high enough for detection at the mid section. This protein level observation is graphically displayed in **Figure 13**.

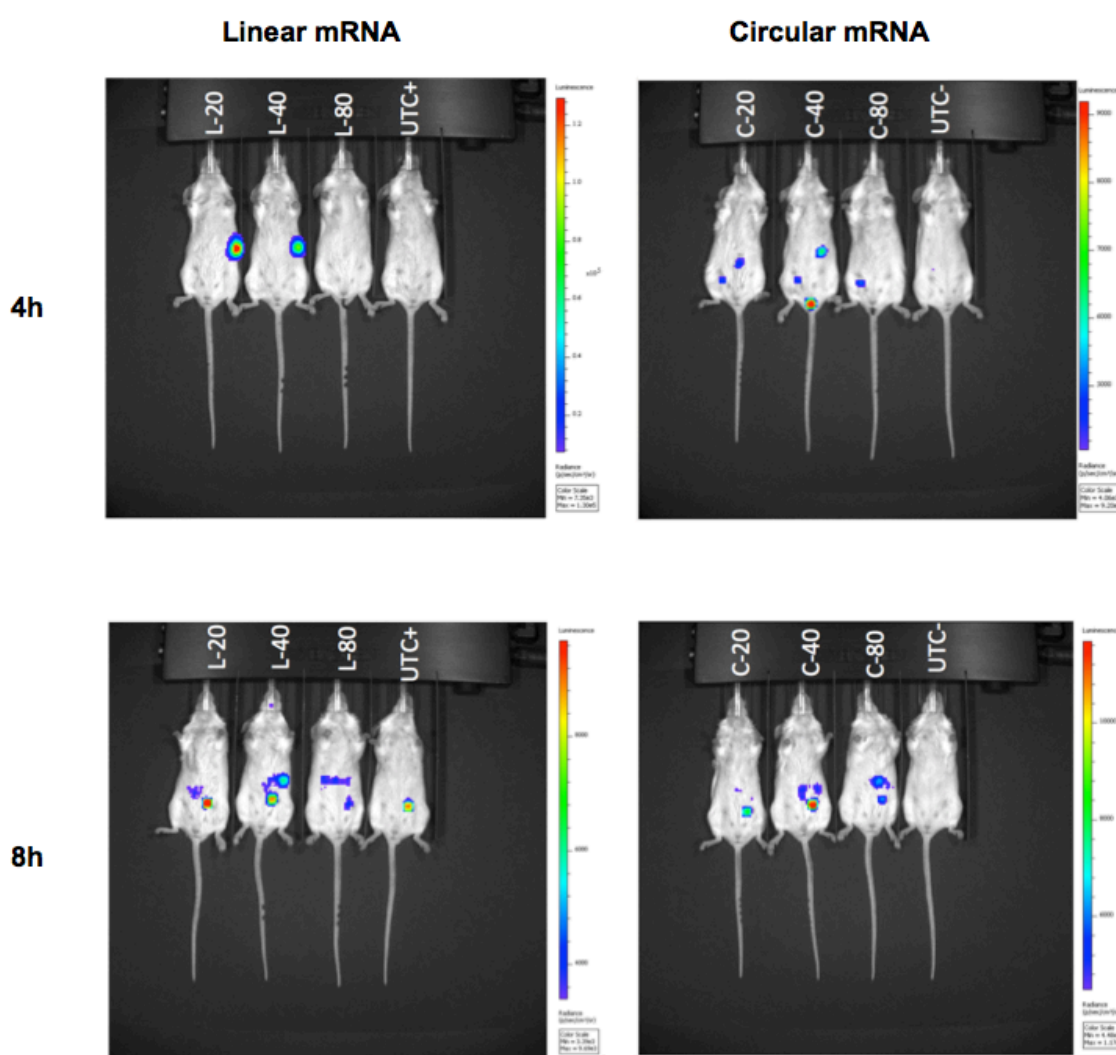


Figure 12 IVIS 4 hours and 8 hours post linear or circular mRNA treatment. Different dosages (20 μ g, 40 μ g, 80 μ g) of linear (L) and circular (C) mRNA were applied to inject mice *i.v.*

Average radiance per mouse decreased to 13-fold and 26-fold for linear mRNA at concentrations 20 μ g and 40 μ g dosage, respectively (**Figure 13, A**). Using 80 μ g linear mRNA treated mice, an increase of 9-fold of average radiance was assessed between the time points 4 hours and 8 hours post injection. However, the increased Nluc level of the 80 μ g linear mRNA treated mouse is similar to the 20 μ g treated mouse at 8 hour after introducing linear nucleic acid encoding Nluc.

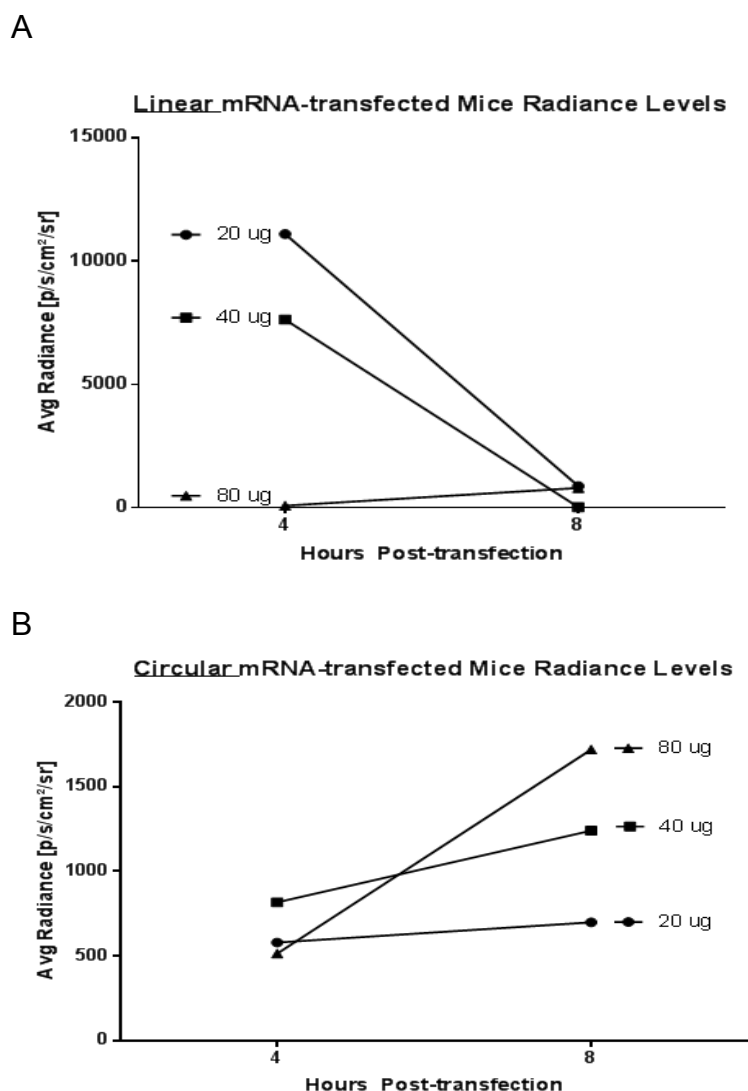


Figure 13 IVIS 4h and 8h time point experiment. The graphical display of average radiance are shown, For linear mRNA a negative and for circular mRNA a positive trend can be determined over the time course.

In contrast to linear mRNA, circular mRNA provides a positive trend during the observed time period with all dosages (**Figure 13, B**). When comparing data from time point 8 hours to 4 hours the greatest increase was observed with a dosage of 80 μ g (3.3-fold), followed by 40 μ g (1.5-fold), and 20 μ g (1.2-fold). Even though Nluc levels from circular mRNA treated mice were associated with a positive trend, in contrast to linear mRNA injected mice, 8 hours post injection the amount of detectable Nluc protein Nluc expression were similar.

Furthermore, after 8 hour IVIS analysis, mice were sacrificed and their liver analyzed to investigate the absolute copy number of linear and circular mRNA, respectively. The result reflected the IVIS finding, suggesting that both types of mRNA have similar mRNA levels after 8 hours, except for 40 μ g circular mRNA treated as it had 2×10^6 more absolute mRNA than its linear counterpart.

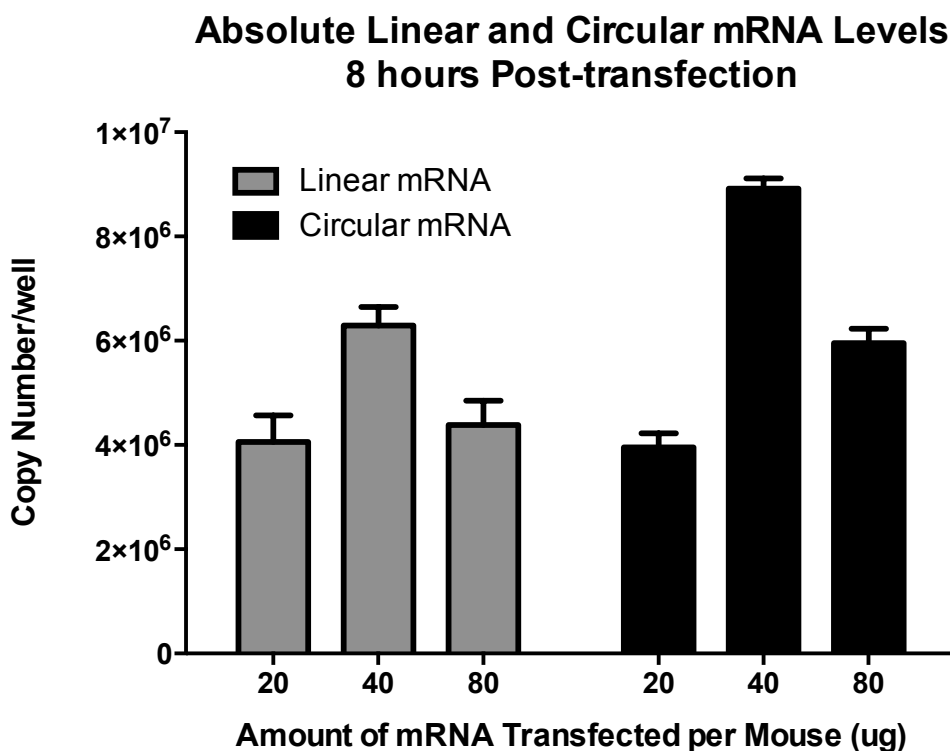


Figure 14 Absolute copy numbers after 8 hours of circular and linear i.v. injection. Error bars indicate standard deviation of triplicate.

3.2.6 Flow cytometry detected Flag-protein, translated from circular mRNA, suggested to lead to a stronger expression after 24 hours in comparison to linear mRNA derived Flag, however, no difference after three days assessed

We next explored the mRNA and protein expression throughout a three-day time course in liver tissue cells. In this experimental set-up, each day – time points 24, 48 and 72 hours post injection (20 μ g mRNA; 7 μ l TransIT-mRNA) – a mouse, which was treated with circular or linear pilot construct on day 0, was sacrificed. Then, its liver tissue cells were isolated without Percoll hepatocyte enrichment and analyzed through flow cytometry and qPCR.

Figure 15 depicts the flow cytometry result as a heat map graph, whereas yellow color indicates high Flag-FITC detection and blue color a low protein detection level. Different Flag-FITC and isotype antibody volume per 200 μ l intracellular staining buffer were applied (1 μ l and 2.5 μ l) to investigate at which concentration best results were obtained. Isotype controls did not emit any signal with both concentrations. 2.5 μ l/200 μ l Flag-FITC antibody provided higher fluorescence readings and its result were also plotted as % of Flag-tag positive cells (**Figure 16**).

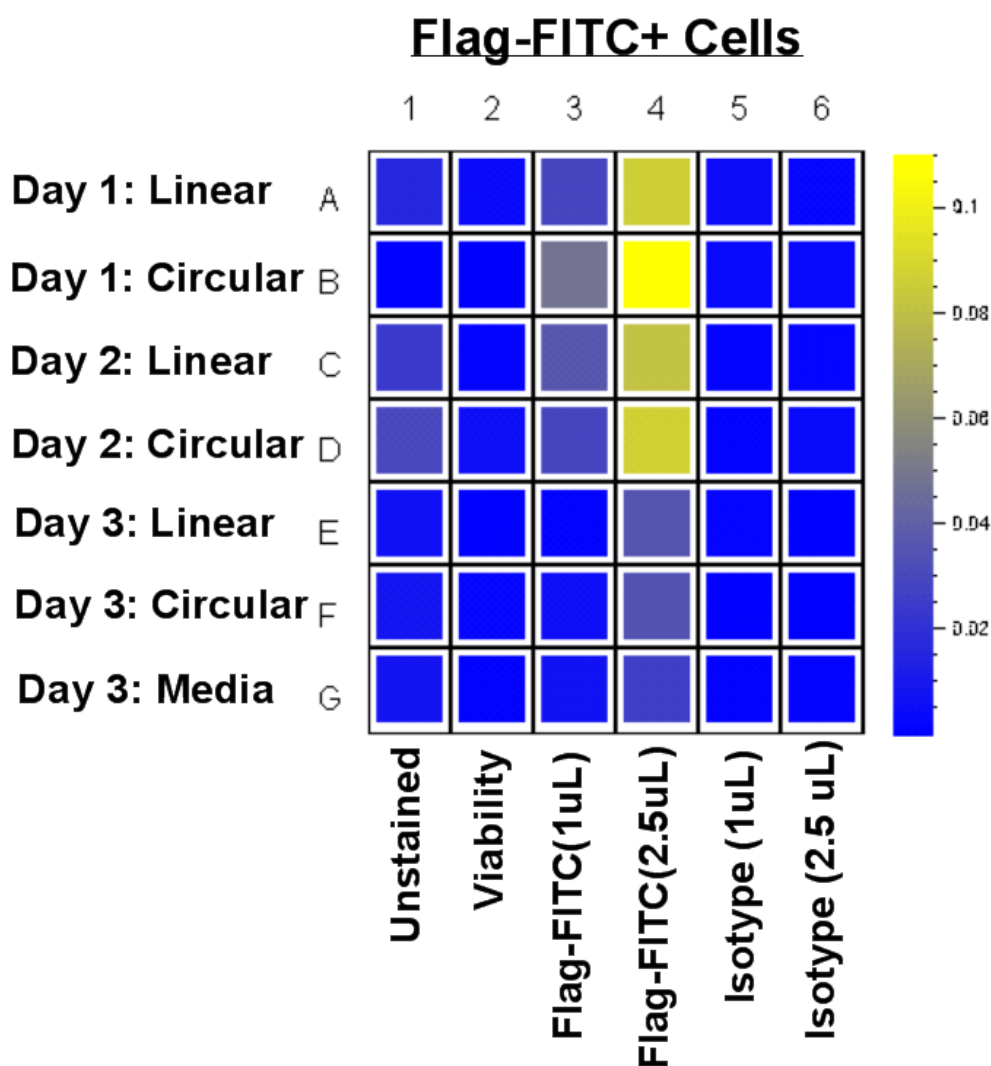


Figure 15 Heat-map of Flag-tag positive cells during a time course of 3 days. Circular mRNA derived Flag protein shows highest detectable level after 1 day.

Figure 16 visualizes the positive Flag-tagged cells in percentage of whole analyzed liver tissue population per mouse treated with either linear or circular mRNA. On day 1 circular mRNA derived 3xFlag-tag was expressed 2.3% more than its linear counterpart. On day 2 and day 3 the difference was diminished and differed by 0.6% and -0.7%, respectively.

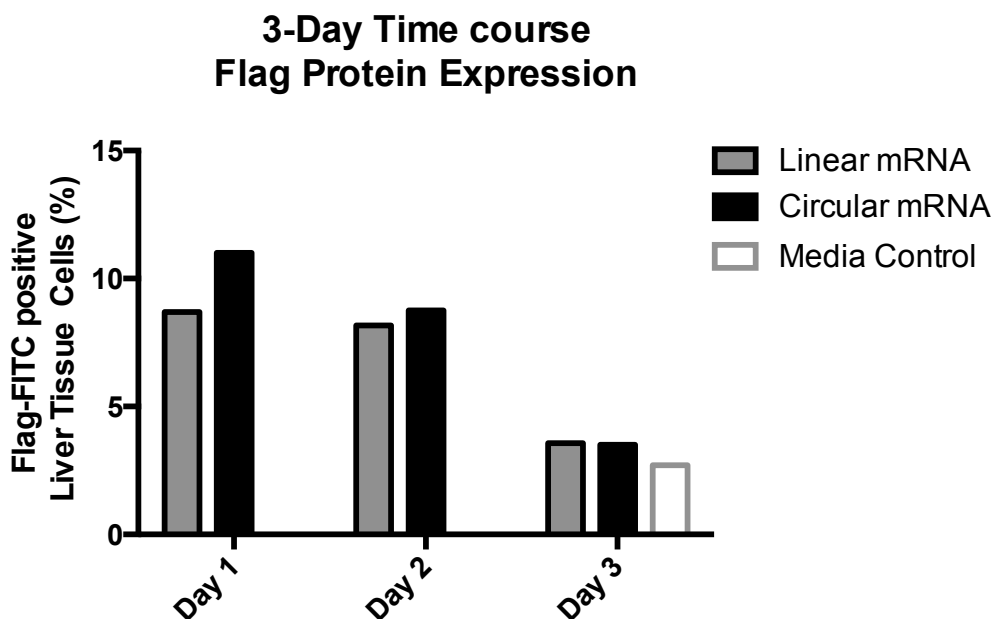


Figure 16 Flag-tag intracellular protein expression in percentage of cell population. Circular mRNA lead to 2.3% higher flag-FITC positive cell population than linear mRNA after 1 day of injection.

3.2.7 Circular mRNA levels associated with sustained stability in murine liver in comparison to canonical linear mRNA in 3-day time course experiment

The 3-day time course study (section 3.2.6) was used to determine for pharmacokinetics protein expression and, in parallel, to identify absolute mRNA copy numbers. The result (**Figure 17**) indicated that 24 hours after i.v. treatment, mRNA levels with circular confirmation had 3 times higher copy numbers than linear mRNA in murine liver.

Interestingly, linear mRNA dropped from day 1 to day 2 by 68%, whereby circular mRNA copy numbers decreased by 18% and remained approximately at the same level on the third day post injection (2% decrease).

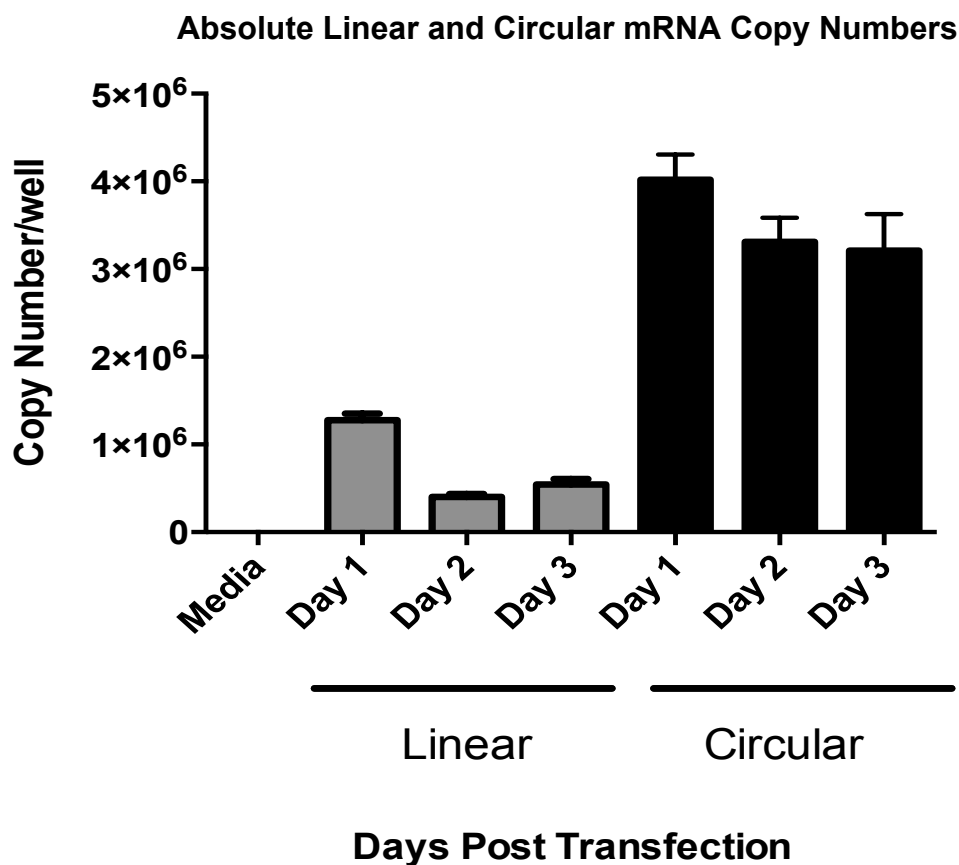


Figure 17 Absolute mRNA level in murine liver during 3-day time course. Linear mRNA copy numbers are and circular transfection. Error bar indicate standard deviation of triplicate.

3.2.8 Hydrodynamic injection led to higher level of protein expression than standard i.v. injection

To possibly increase transfection efficiency of liver cells we then also investigated the effect of hydrodynamic injection in comparison to standard i.v. injection. For this experiment, linear and circular mRNA were injected either in a volume of 1ml or 200 μ l with or without TranIT-mRNA transfection reagent. Nluc expression and distribution through in vivo imaging of time points of 4, 8, 24, and 72 hours post-injection were investigated (**Figure 18, Figure 19**).

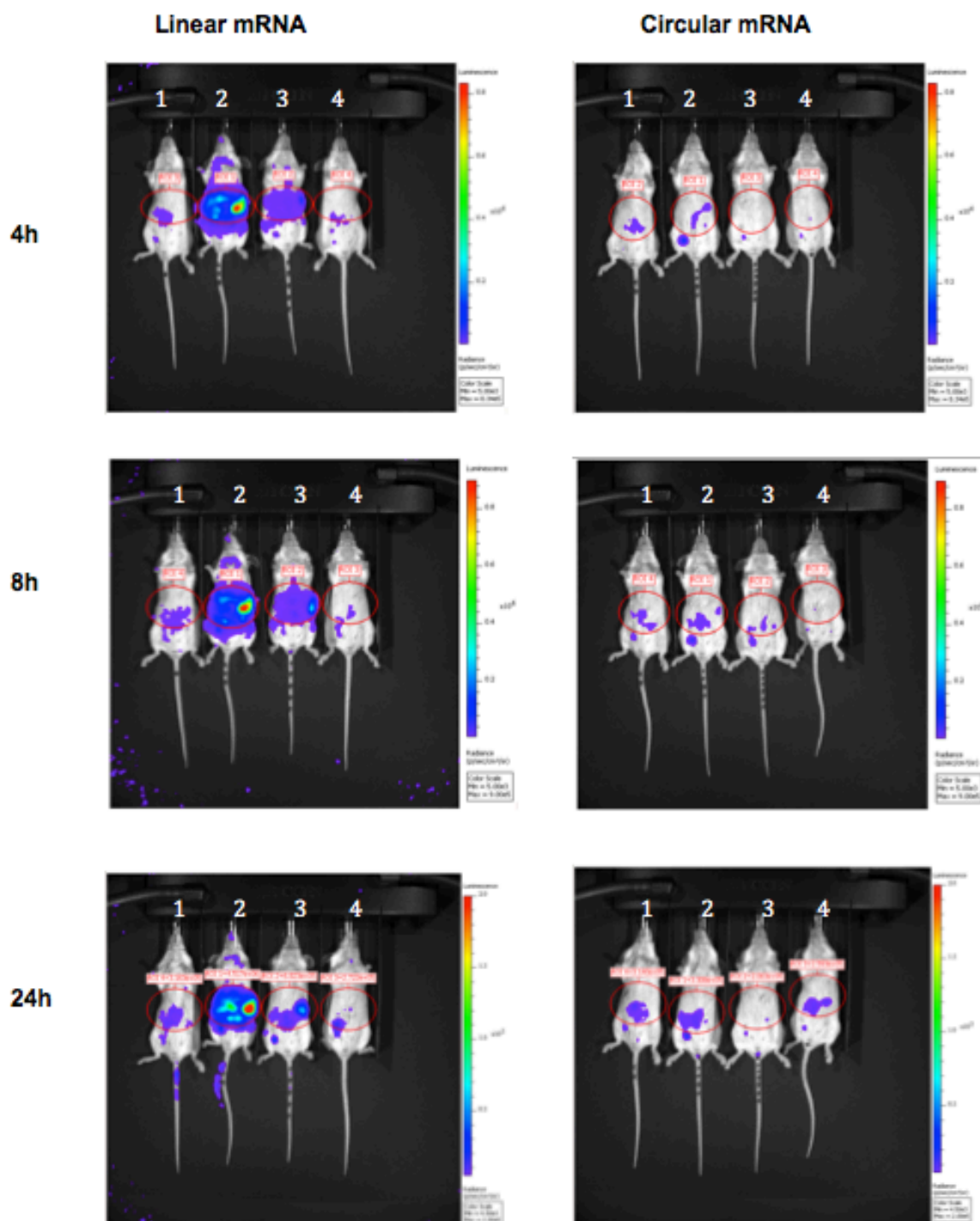
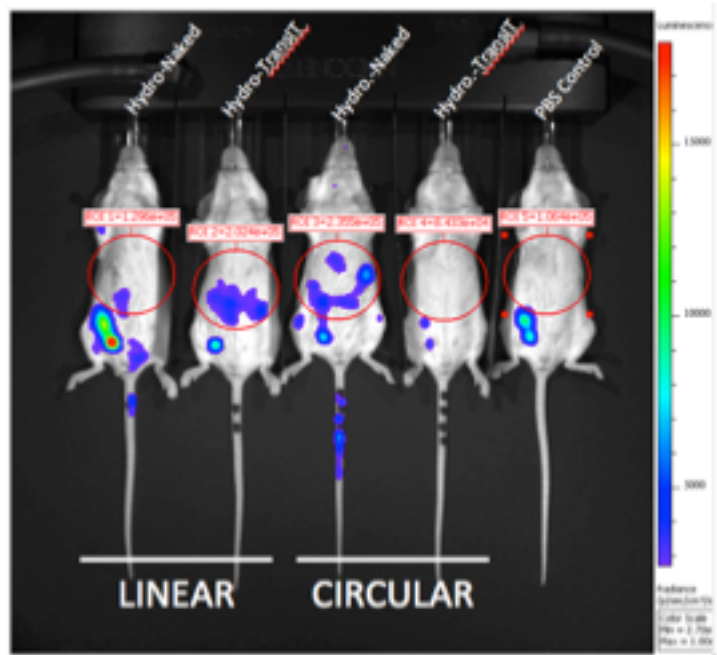


Figure 18 *IVIS hydrodynamic and standard i.v. injection in comparison. Higher signal levels obtained with linear mRNA treatment than with circular mRNA. 1:Hydrodynamic injection without transfection reagent; 2: Hydrodynamic injection with TransIT-mRNA; 3: Standard injection with TransIT-mRNA 4: Standard injection control with PBS.*

A

72h



B

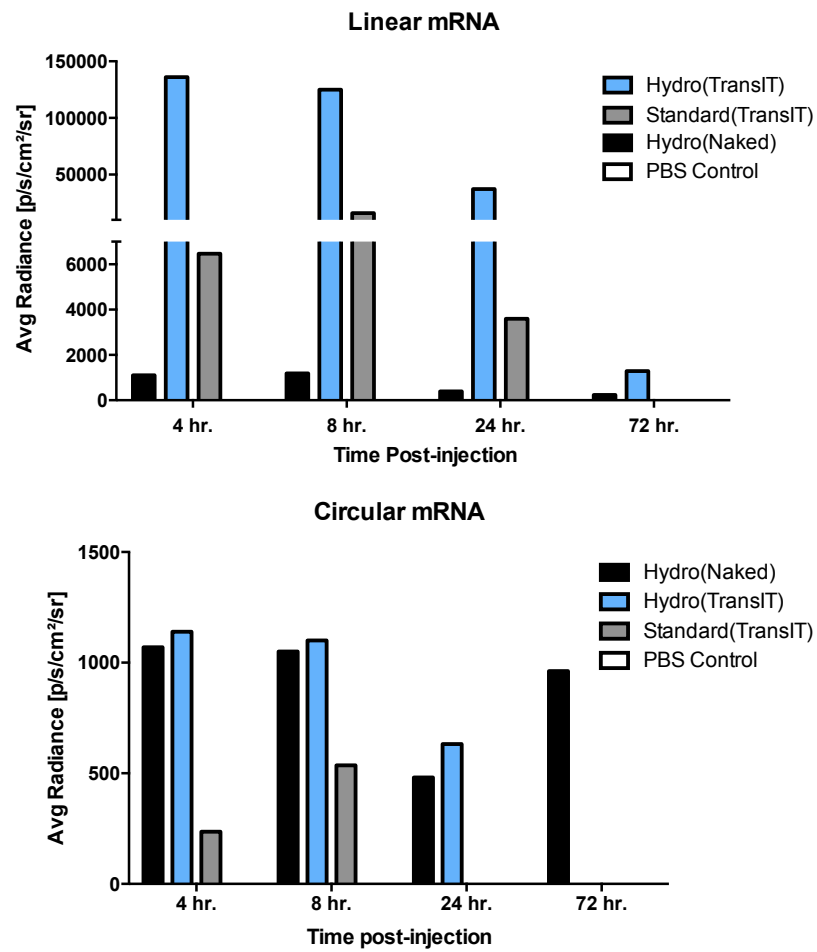


Figure 19 IVIS hydrodynamic and standard i.v. injection in comparison (cont.).
 (A) 72h in vivo imaging of hydrodynamic and standard i.v. injection (B) Graphical comparison of average radiance of all time points. Each bar represents one mouse

In this three-day time course experiment, hydrodynamic injection with TransIT-mRNA led to a 21-fold increase of Nluc signal detection for linear mRNA treated mice in comparison to standard i.v. TransIT-mRNA mediated nucleic acid transfection. However, hydrodynamically injected naked linear mRNA, thus not complexed to a transfection reagent, resulted in 124-fold less signal. This was a similar signal range hydrodynamically injected circular mRNA was detected.

From the obtained IVIS signal result we then compared the stability of Nluc proteins derived from linear or circular mRNA introduced systemically via the tail vein route with hydrodynamic injection with or without transfection reagent TransIT-mRNA. Thereby, for linear or circular mRNA respectively, 100% was determined as the signal detected 4 hours post TransIT-mRNA hydrodynamic injection (**Figure 20**). Nluc protein expression after linear mRNA injection dropped from 4 to 8 hours by 8%, after 24 hours by another 63%, and diminishes after 72 hours. In contrast for both naked and TransIT-mRNA complexed circular mRNA 24 hours post hydrodynamic injection a 9% drop was detected. After 72 hours, naked mRNA protein expression was still at a level of 66%, whereas complexed with TransIT-mRNA was at 27%.

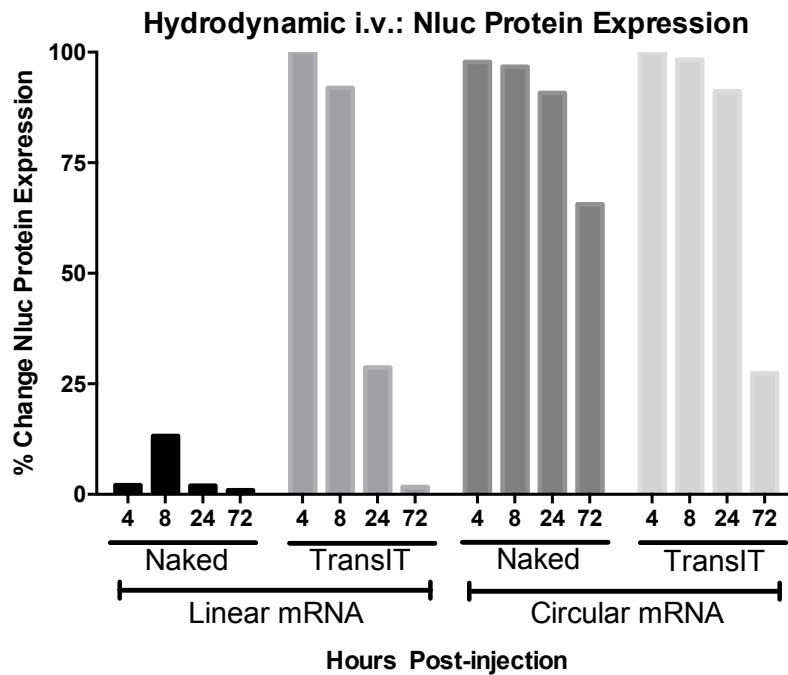


Figure 20 Nluc protein stability of linear and circular mRNA administered via hydrodynamic i.v. injection

4 Discussion

For a number of decades mRNA therapy is gaining ground^{83,12}, as it has demonstrated to be an attractive option due to its versatile application possibilities and advantages as described in the introduction section (1.1 Protein- and Gene Therapy). However, the degradation of mRNA, in particular through the major exonuclease pathway²², is a hindrance for therapeutic applications. Thus, to circumvent degradation at the 3' and/or 5' end of the nucleotide molecule, we hypothesized that circularizing coding mRNA will lead to a more stable mRNA molecule, increasing translation of the protein of interest.

This master project sought to characterize pharmacokinetics of circular mRNA *in vivo*. Thereby, we compared enzymatically circularized reporter mRNA, encoding Nluc and 3xFlag-tag with its linear counterpart. Our results demonstrate stability differences on mRNA and protein level between linear and circular mRNA, favorable to the latter.

4.1 Linear and circular mRNA constructs

mRNA bears many advantages such as no insertional mutagenesis, relatively easy to engineer, and, being a cytoplasmic expression system, allows this approach to transfect even quiescent or slowly proliferating host cells¹². However, for mRNA therapy to succeed, two challenges have to be overcome: immunogenicity¹⁴ and instability¹². This work focuses on the latter caveat. Even though chemically modified mRNA had been shown to increase time for protein translation¹⁴, there is a need to develop efficient strategies to further enhance mRNA stability for therapeutic utility.

Linear mRNA are susceptible of degradation pathways, of which exonuclease degradation is the major reason for mRNA decay⁸⁴. Interestingly, endogenous circular transcripts were identified in nature⁸⁵ and are found to be stable²⁸. Thus, we hypothesized that circular mRNA exhibit enhanced stability can be utilized to

prolong protein expression and therefore this concept can be used for therapeutic settings.

To assess pharmacokinetics of circular mRNA *in vivo*, we therefore generated a reporter construct encoding Nluc and 3xFlag-tag, which we then circularized. Through extensive prior work of PhD candidate Ellese Carmona, a protocol using enzymatic circularization based on the work of Beaudry and Perrault³⁹ was evaluated as the most efficient circularization method and had been used for these experiments. For verification, linear and circular mRNA were subjected to gel electrophoresis. For circular mRNA, two bands were visible on the gel, whereas the upper slower migrating band was the circularized product (**Figure 4**), similar to the result Beaudry and Perrault obtained³⁹.

Outward oriented PCR²⁶ was another technique we approached to ensure circular conformation of our construct. Indeed, with this method we obtained the sequence of a 5' to 3' junction, which would not have resulted with linear mRNA (**Figure 5**).

The first pilot *in vivo* studies were initiated to investigate whether using circular mRNA results in changed pharmacokinetic characteristics in comparison to linear mRNA.

4.2 Establishment of *in vivo* study

To use mRNA as a therapeutic for type I diabetes, the liver was targeted as protein synthesis platform for our exogenous mRNA. Particularly, as the liver bears great capacity in protein synthesis and secretion^{86,87,88}. Additionally, extrapancreatic proinsulin-producing cells were also found in the liver of streptozotocin-induced diabetic mice, *ob/ob* mice, and mice fed a high fat diet.⁶⁶ Here, intravenous injection into the tail vein was used to administer the mRNA constructs to target the liver. Importantly, this allows the mRNA-solution to be directly administered as a bolus into the blood⁸⁹. Furthermore, the liver has a high blood flow⁸⁸, facilitating improved uptake of intravenously injected mRNA.

To elevate transfection efficiency for our experiment, four commercially available transfection reagents (InvivoFectamin 3.0, Turbofect, Lipofectamine RNAiMAX, TransIT-mRNA) were tested to complex the constructed reporter mRNA to improve the transfection efficiency. By analyzing Nluc mRNA as a gauge for mRNA translation, we found that TransIT-mRNA was the best transfection reagent candidate for efficiently targeting liver tissue with our linear mRNA construct. In contrast to the mRNA without transfection reagent control, a 3×10^5 fold higher level was detected using mRNA complexed with TransIT-mRNA. No difference in complexing the transfection reagent with linear or circular mRNA was expected, and thus only linear mRNA was tested to determine the optimal transfection reagent. Turbofect was the second best transfection reagent with a 2×10^3 higher relative level of Nluc mRNA than the control. The other two transfection reagents (InvivoFectamin 3.0 and RNAiMax) gave negligible mRNA transfer. Focusing on the protein expression, TransIT-mRNA was the most efficient transfectant, demonstrating a 6-fold improvement compared to the next best transfection reagent. Interestingly, mRNA introduced systemically with Turbofect yielded in low translated Nluc protein level, whereas InvivoFectamin 3.0 and RNAiMax performed better (approx. 25RLU) (**Figure 6**). TransIT-mRNA, a cationic polymer/lipid formulation, forms non-liposomal micelles to transfect the cells of interest with mRNA. Although TransIT-mRNA yielded high transfection efficiency, toxicity in mice was also significant. The mice injected with this transfectant either died immediately after administration or displayed lethargic breathing, requiring several minutes under a heat lamp to recover from the toxic effect. TransIT-mRNA was developed for *in vitro* use, which may explain its toxicity, and specific *in vivo* administration of the reagent was not recorded by the manufacturer. However, promising results with TransIT-mRNA have also been noted by other groups through personal communication. Furthermore, other studies have reported that TransIT-mRNA could be successfully used *in vivo* to complex mRNA but when administered intraperitoneally⁹⁰. As the components of TransIT-mRNA are under proprietary rights, we were unable to determine the exact cause of its toxicity. We tested the pH of the solution, but this was neutral, and therefore should not have had any toxic effect on the animals. Furthermore, following *i.v.* injection, the

neutral pH of the blood would cause a dilution effect through the blood flow and the buffering of blood itself⁹¹. On the basis of the mentioned findings, we concluded TransIT-mRNA as the best transfection reagent and continued with investigating the optimal, non-toxic dosage for tail vein *i.v.* injection into mice.

Our initial experiments had shown that TransIT-mRNA produced lethal or severe side-effects at a volume of 28 μ l. Therefore, titration experiments were conducted to determine the dose that was not toxic to the animals as well as providing reliable transduction. TransIT-mRNA was tested in four decreasing amounts (in 25% increments of maximum tolerated TransIT-mRNA volume): 8 μ l, 14 μ l, 21 μ l and 28 μ l. Following the injection of the 200 μ l mRNA mixture bolus containing 21 μ l TransIT-mRNA, adverse reactions were observed as mice experienced breathing problems and were reluctant to move. However, this appeared to be transient and ceased after several minutes. As adverse responses were observed at this amount, the 28 μ l injection of TransIT-mRNA was not administered. We then analyzed the Nluc mRNA level relative to RNAiMAX treated mice (**Figure 7,A**). Maintaining the same mRNA dosage, an increase of Nluc mRNA was detected using qPCR which increased proportionately at the TransIT-mRNA volume used. This is most likely because more transfectant reagent can complex greater amounts of mRNA, facilitating entry into the cytoplasm of the hepatocytes. Nluc protein expression mirrored the mRNA level results (**Figure 7, B**). Except for the highest volume, a direct proportional trend can be found. This might indicate that after a certain mRNA/transfectant ratio, an indirect proportional relation of transfection efficiency might occur *in vivo*. In regards to toxicity, we could thus determine that TransIT-mRNA with 20 μ g mRNA should not exceed 21 μ l TransIT-mRNA reagent volume in *i.v.* setting. Using 14 μ l TransIT-mRNA volume in this experiment, the ratio was 1.4 μ g mRNA / 1 μ l TransIT-mRNA reagent and 0.5 μ l Boost. Previously, Kariko et. al. published data using the same transfection reagent *in vivo* for their intraperitoneal injection in mice.⁹⁰ Their applied ratio of mRNA to reagent was different than ours (1 μ g mRNA/1.1 μ l TransIT-mRNA reagent, 7 μ l Boost) injecting 0.1 μ g mRNA encoding erythropoietin (EPO) *i.p.* to measure an increase in EPO circulating in blood.

4.3 Ex-vivo 3xFlag-tag detection for linear and circular mRNA treated mice

The principle of circular mRNA for clinical treatment in humans has a potential to be applied to a plethora of diseases such as cancer and Type I Diabetes. As proof of principle, this project focused on Type I Diabetes, using circular mRNA encoding preproinsulin. To monitor the presence of cleaved exogenous preproinsulin, thus proinsulin⁹², a 3xFlag will be cloned into its C-terminal site. Hence, it was crucial to find a suitable method to detect the 3xFlag-tag from our reporter construct. Westernblotting, an analytical technique to detect and compare protein expression through specific antibodies¹⁵, was first used to measure 3xFlag expression in the liver tissue of mice transfected with mRNA. Whole liver tissue lysates were probed with monoclonal anti-Flag antibody, however, only the commercially available Flag positive control was detected. The same antibody was previously reported to bind to 3xFlag-tagged proteins of interest in mouse tissue^{93,94}. However, we were unable to detect any signals despite positive signals from the control (**Figure 8, upper panel**). Upon increased exposure of the blot, unspecific bands were visible in the negative control. This crosslinking might be caused by the antibody being raised in mice and thus its constant Fc region may unspecifically bind to mouse protein samples as well. Thus, polyclonal antibodies from rabbit hosts were probed, but as with the Nluc antibody no signals were detected either (Data not shown). To ensure equal protein load per well, expression of beta actin was assessed (**Figure 8, lower panel**). All the assessed tissue samples had bands at the size of Beta actin, 42kDA. Only the Flag positive control did not give any signal as it was a commercially obtained purified FLAG-BAP fusion protein.

3xFlag-tag has a superiority over single Flag-tag epitope system and is detectable in samples upto 10 fmol⁶⁹. However, westernblotting only allows whole liver cell population being analyzed together on a blot, leading to less sensitive assessment than with single cell analyses approach used in flow cytometry. Flow cytometry detects properties of single cells through fluorescence emission and optical measurements. Using forward angle light scatter, physical characteristics like cell

size is determined. Furthermore, fluorescent dyes conjugated to antibodies can specifically bind to proteins of interest in the cytoplasm or on the cell membrane. The basic principle behind flow cytometry is that once the single cell passes the light beam with its excitation wavelength, the fluorochrome elevates to a higher energy level. When the fluorophore returns to its basic energy level, light is emitted at higher energy wavelengths. The light signal is detected by photomultiplier tubes and converted to be used for computational analyses⁹⁵. Thus, to determine Flag-tag on a single cell basis we used an anti-flag antibody conjugated with the fluorophore Fluorescein isothiocyanate (FITC). Further, for our pilot study we applied a Percoll gradient modified from Goncalves et al. for hepatocyte enrichment. We further used the described gating strategy for morphological hepatocyte determination⁹⁶. FITC is a commonly used fluorophore and had been reported to be used in analyzing mouse samples^{97,98}. However, natural fluorescence is also emitted in tissue. Primary sources are reduced NAD(P)H, endogenous flavins, lipofuscins, collagen, elastin and reticulin fibres, which are in particular highly present in liver and kidney tissue. Furthermore, these molecules emit fluorescence at wavelengths between 540 and 650nm, partially overlapping with the emission wavelength of FITC⁹⁹. Thus, untreated hepatocytes should be used as control to deduct these background signals. However, in our pilot flow cytometry result, only 0.3% of the untreated hepatocyte control produced fluorophore signals at the interrogated FITC emission wavelength. Thus, autofluorescence was negligible in our setting. No mRNA control showed 17% of unspecific binding and should be deduced from any signal resulting from treated mice liver. 24 hours post i.v. treatment with circular mRNA, 25% of the hepatocyte population expressed Flag-tag protein. In contrast, 43% of linear mRNA treated murine hepatocyte were Flag-tag positive (**Figure 9**). Moreover, comparing Flag proteins derived from linear mRNA to its circular counterpart displayed that the former lead to a greater population of hepatocytes with higher amount of flag reporter level. This might be due to linear mRNA having a higher translation capacity than circular mRNA. However, if circular mRNA indeed exhibits higher stability than linear mRNA, circular mRNA will lead to a prolonged expression of proteins.

4.4 IVIS: Nluc protein biodistribution after standard i.v. injection

Unlike many assessment options, *in vivo* imaging is not an endpoint analysis and allows continuous protein expression surveillance of one mouse at chosen time points. Thereby, the emitted light of luciferase in reaction with its substrate is harnessed. Here, we take advantage of Nluc, which reacts with the specifically engineered substrate Furimazine generating luminescence⁷⁴. Nluc is derived from a deep-sea shrimp and has a size of 19kDA. Its substrate Furimazine is ATP-independent and thus Nluc can be detected extracellularly as well⁷⁴. Nluc was only recently reported and thus only limited knowledge about its features *in vivo* were known^{70,75,76}. The output we chose here is the average radiance, which is described as the quantity of photons per second emitted from a tissue area of a square centimeter and radiate into one steradian.

mRNA half-life in eukaryotic cells is intrinsic, varies highly and even changes in response to extracellular stimuli¹⁰⁰. The resultant protein expression level is dependent on both, protein synthesis from mRNA as well as its degradation. With flow cytometry we were able to detect Flag-tag antibodies 24 hours post-injection. Thus, we decided to investigate the same time point with *in vivo* imaging of Nluc (**Figure 11**). However, luminescence could not be detected. Signal detection is quantity and protein/tissue depth dependent¹⁰¹. As it was published in other studies to detect Nluc signals deriving from the intestine^{70,75,76}, we focused on altering the time point of analyses, as mRNA and protein half-life might be the limiting factor. Thus, shorter time frames of 4 and 8 hours were chosen (**Figure 12, Figure 13**). After 4 hours, linear mRNA derived Nluc was mostly found in the spleen, similar as described by Phua et al. as they reported to have found nanoparticle coated mRNA at the spleen site as well, post intravenous injection⁸². After 8 hours Nluc expression seemed to have cleared from the spleen and was found in the mid section of the mice. Circular mRNA treated mice emitted 10-fold less signal than linear mRNA in the abdominal viscera and at the injection site 4 hours post i.v. administration. After 8 hours, the Nluc protein signal of circular mRNA treated mice increased throughout all observed dosages. Although, after 8 hours both linear and circular mRNA treated mice showed similar Nluc protein

expression, linear mRNA was associated with a negative trend, whereas for circular mRNA derived reporter protein a positive trend was distinguishable. Longer time periods could verify these findings, and other organs (*i.e.* spleen, pancreas) could be subjected to *ex vivo* Nluc or Flag-tag analyses as well.

4.5 Circular mRNA associated with beneficial protein and mRNA stability over a time course of 3 days

We then prolonged the study period to three days to investigate the protein expression on a single cell basis through flow cytometry. In parallel, absolute mRNA expression of circular and linear mRNA treated mice was also determined. In contrast to the previous flow cytometry experiment, we included other cell types of the liver too, as no Percoll gradient was applied. For three consecutive days after every 24 hours, one mouse was sacrificed and liver subjected to analyses. On protein level (**Figure 15, Figure 16**), cells of liver tissue derived from circular mRNA treated mice were associated with stronger 3xFlag-tag expression than their linear counterpart mice group after 1 day. However, this difference diminishes on day 2. On day 3 no difference in protein expression was apparent.

Interestingly, comparing hepatocyte non- and enriched samples after 24 hours, a shift between which form of mRNA yielded in higher 3xFlag-tag protein expression became evident. Indeed, mRNA delivery is a stochastic process and a variation of expression level can be found in every cell⁴⁴. Applying a Percoll gradient (**Figure 9**) or omitting gradient centrifugation (**Figure 15-Figure 17**) results in different cell population, as Percoll gradient enriches hepatocytes⁹⁶. Hence, in our three-day time course study, more non-hepatocytes were included in the analyzed cell population. This may be the cause of a shift towards elevated expression of circular mRNA-derived proteins in comparison to linear mRNA-derived proteins. However, subtracting background signal (media control), 3xFlag-tag expression was found in below 10% of the cell population. In contrast, enriching hepatocytes with Percoll gradient lead to 3xFlag-tag protein expression found in 25.5% (circular mRNA treated) and 43% (linear mRNA treated) of cell population. Thus,

hepatocytes were transfected most with mRNA and for future experiments hepatocyte enrichment with Percoll gradient would be necessary to investigate the pharmacokinetic characteristics in these types of cells. Staining with different cell markers could be used next to phenotype the cell types expressing the most exogenous protein derived from introduced constructs.

Moreover, in foresight that insulin will be the therapeutic protein to be expressed, the chosen target tissue was the liver. Interestingly, it had been found that in the liver of diabetic mice, proinsulin and insulin producing cells were present⁶⁶. However, even though a majority of the liver tissue indeed consist of parenchymal liver cells (67%)¹⁰², phenotyping had not been performed in the mentioned study. Other cell type present in the liver are endothelial cells, fat-storing cells, Kupffer cells (liver macrophages), and pit cells (natural killer cells)^{103–105}. These mentioned cells, termed sinusoidal cells, may either negatively effect or positively contribute to some degree to the exogenous protein production.

Strikingly, in respect to mRNA level, the three-day time course study demonstrated that circular mRNA elicited a three-fold overall higher level than linear mRNA in liver tissue. Additionally, circular mRNA was resistant to degradation unlike its linear counterpart, demonstrated by 68% loss of the latter after 1 day, in contrast to only 18% degradation of circular mRNA. The cause for this indeed may be that circular mRNA can longer evade exonuclease degradation.

4.6 Hydrodynamic injection led to higher detected Nluc signal

Furthermore, attempting to increase transfection efficiency in liver, we approached hydrodynamic injection with naked or TransIT-mRNA as transfectant complexed mRNA. Hydrodynamic injection through the tail vein is an emerging approach using rapid high volume injection to achieve hepatocyte transfection with DNA or RNA^{51,106}. To transfect the liver with mRNA using this technique had been successfully shown by McCaffrey *et al.*¹⁰⁷, Wilber *et al.*¹⁰⁸ and Crowley *et al.*¹⁰⁶. In these experiments, the more common firefly luciferase enzyme and its substrate

luciferin were used for detection. Moreover, RNase inhibitor and decoy RNA had been applied to competitively bind to RNases found in blood and extracellular space^{107,108}. Polyethylene glycosylated polyacridine peptide was another approach to escape mRNA instability¹⁰⁶.

We used Nluc and furimazine to detect via *in vivo* bioluminescence imaging pharmacokinetic of proteins derived from linear or circular mRNA at time points 4, 8, 24, and 72 hours (**Figure 18**, **Figure 19**). Thereby, for circular mRNA hydrodynamic injection led to 5-fold increased transfection efficiency in comparison to standard *i.v.* injection, shown by the subsequent translation of Nluc protein. For linear mRNA, both standard and hydrodynamic injections, in which the nucleic acid was complexed with transfection reagent, were superior over hydrodynamic naked mRNA transfection approach.

Focusing on protein stability (**Figure 20**), Nluc protein expression of circular mRNA treated mice, decreased only by 9% after 24 hours of injection in both naked and TransIT-mRNA mediated hydrodynamic injection. In contrast, linear mRNA treated mouse with transfection reagent reduced its protein expression by 71% at 24 hours post-injection. Interestingly, hydrodynamic naked linear mRNA did not lead to efficient transfection of liver cells in comparison to complexed with transfection reagent. Naked mRNA may have been subjected to of RNases found in abundance in extracellular space and blood-stream¹⁰⁷. However, circular naked mRNA escaped this degradation and led to protein expression similar to that of circular mRNA complexed with aiding transfection reagent. This suggests that circular mRNA are more resistant to nucleases than linear mRNA.

As circular mRNA had shown promising result in more stable protein expression over time, future approaches could involve further modification of circular mRNA to increase protein translation efficiency *in vivo*.

5 Conclusion

Our pilot *in vivo* study shed light into the pharmacokinetics characterization of circular mRNA. We were able to identify suitable detection methods for our first experiments performed in mice, both on mRNA and protein level. Collectively to this end, our encouraging results suggest that circular mRNA levels are more stable than linear mRNA during a three-day time course. Proteins derived from circular mRNA are associated with a beneficial stability in comparison to linear mRNA.

Further extensive research is in need to be conducted to manifest whether circular mRNA is indeed demonstrating a significantly increased stability than canonical linear mRNA, thus, enabling a prolonged protein expression leading to circular mRNA to emerge as a novel template for therapeutic gene transfer for various maladies.

List of References

1. Soto, C. Unfolding the role of protein misfolding in neurodegenerative diseases. *Nat. Rev. Neurosci.* **4**, 49–60 (2003).
2. Leader, B., Baca, Q. J. & Golan, D. E. Protein therapeutics: a summary and pharmacological classification. *Nat. Rev. Drug Discov.* **7**, 21–39 (2008).
3. Valastyan, J. S. & Lindquist, S. Mechanisms of protein-folding diseases at a glance. *Dis. Model. Mech.* **7**, 9–14 (2014).
4. Rekitke, N. E., Ang, M., Rawat, D., Khatri, R. & Linn, T. Regenerative Therapy of Type 1 Diabetes Mellitus: From Pancreatic Islet Transplantation to Mesenchymal Stem Cells. *Stem Cells Int.* **2016**, 3764681 (2016).
5. Putney, S. D. & Burke, P. A. Improving protein therapeutics with sustained-release formulations. *Nat. Biotechnol.* **16**, 153–157 (1998).
6. Mahmood, I. & Green, M. D. Pharmacokinetic and pharmacodynamic considerations in the development of therapeutic proteins. *Clin. Pharmacokinet.* **44**, 331–47 (2005).
7. Schellekens, H. Bioequivalence and the immunogenicity of biopharmaceuticals. *Nat. Rev. Drug Discov.* **1**, 457–62 (2002).
8. Beck-Sickinger, A. G. & Mörl, K. Posttranslational Modification of Proteins. Expanding Nature’s Inventory. By Christopher T. Walsh. *Angew. Chemie Int. Ed.* **45**, 1020–1020 (2006).
9. Gross, M. L. Ethics, Policy, and Rare Genetic Disorders: The Case of Gaucher Disease in Israel. *Theor. Med. Bioeth.* **23**, 151–170
10. Wirth, T., Parker, N. & Ylä-Herttuala, S. History of gene therapy. *Gene* **525**, 162–9 (2013).
11. Sahin, U., Karikó, K. & Türeci, Ö. mRNA-based therapeutics — developing a new class of drugs. *Nat. Rev. Drug Discov.* **13**, 759–780 (2014).

12. Tavernier, G. *et al.* mRNA as gene therapeutic: how to control protein expression. *J. Control. Release* **150**, 238–47 (2011).
13. Mclvor, R. S. Therapeutic delivery of mRNA: the medium is the message. *Mol. Ther.* **19**, 822–3 (2011).
14. Kormann, M. S. D. *et al.* Expression of therapeutic proteins after delivery of chemically modified mRNA in mice. *Nat. Biotechnol.* **29**, 154–157 (2011).
15. Alberts, B. *et al.* *Molecular Biology of the Cell. Amino Acids* **54**, (Garland Press, 2008).
16. Pray, L. Discovery of DNA Structure and Function: Watson and Crick. (2013).
17. WATSON, J. D. & CRICK, F. H. C. Molecular Structure of Nucleic Acids: A Structure for Deoxyribose Nucleic Acid. *Nature* **171**, 737–738 (1953).
18. Berg JM, Tymoczko JL, S. L. *Biochemistry 5th Edition.* (W H Freeman, 2002).
19. Clancy, S. DNA Transcription. *Nat. Educ.* **1(1):41**, (2008).
20. White, R. J. Transcription by RNA polymerase III: more complex than we thought. *Nat. Rev. Genet.* **12**, 459–63 (2011).
21. Izban, M. G. & Luse, D. S. Factor-stimulated RNA polymerase II transcribes at physiological elongation rates on naked DNA but very poorly on chromatin templates. *J. Biol. Chem.* **267**, 13647–55 (1992).
22. Schoenberg, D. R. & Maquat, L. E. Regulation of cytoplasmic mRNA decay. *Nat. Rev. Genet.* **13**, 246–59 (2012).
23. Garneau, N. L., Wilusz, J. & Wilusz, C. J. The highways and byways of mRNA decay. *Nat. Rev. Mol. Cell Biol.* **8**, 113–26 (2007).
24. Liu, Y. *et al.* Construction of circular miRNA sponges targeting miR-21 or miR-221 and demonstration of their excellent anticancer effects on malignant melanoma cells. *Int. J. Biochem. Cell Biol.* **45**, 2643–50 (2013).

25. Li, J. *et al.* Circular RNAs in cancer: novel insights into origins, properties, functions and implications. *Am. J. Cancer Res.* **5**, 472–80 (2015).
26. Jeck, W. R. & Sharpless, N. E. Detecting and characterizing circular RNAs. *Nat. Biotechnol.* **32**, 453–61 (2014).
27. Jeck, W. R. & Sharpless, N. E. Detecting and characterizing circular RNAs. *Nat. Biotechnol.* **32**, 453–61 (2014).
28. Jeck, W. R. *et al.* Circular RNAs are abundant, conserved, and associated with ALU repeats. *RNA* **19**, 141–157 (2012).
29. Qu, S. *et al.* Circular RNA: a new star of noncoding RNAs. *Cancer Lett.* **365**, 141–148 (2015).
30. Zhang, Y. *et al.* Circular intronic long noncoding RNAs. *Mol. Cell* **51**, 792–806 (2013).
31. Li, Z. *et al.* Exon-intron circular RNAs regulate transcription in the nucleus. *Nat. Struct. Mol. Biol.* **22**, 256–64 (2015).
32. Wang, Y. & Wang, Z. Efficient backsplicing produces translatable circular mRNAs. *RNA* **21**, 172–9 (2015).
33. Li, F. *et al.* Circular RNA ITCH has inhibitory effect on ESCC by suppressing the Wnt/ β -catenin pathway. *Oncotarget* **6**, 6001–13 (2015).
34. Hansen, T. B., Kjems, J. & Damgaard, C. K. Circular RNA and miR-7 in cancer. *Cancer Res.* **73**, 5609–12 (2013).
35. Burd, C. E. *et al.* Expression of linear and novel circular forms of an INK4/ARF-associated non-coding RNA correlates with atherosclerosis risk. *PLoS Genet.* **6**, e1001233 (2010).
36. Moore, M. J. & Query, C. C. Joining of RNAs by splinted ligation. *Methods Enzymol.* **317**, 109–23 (2000).
37. Perriman, R. Circular mRNA encoding for monomeric and polymeric green fluorescent protein. *Methods Mol. Biol.* **183**, 69–85 (2002).

38. Perriman, R. & Ares, M. Circular mRNA can direct translation of extremely long repeating-sequence proteins in vivo. *RNA* **4**, 1047–54 (1998).
39. Beaudry, D. & Perreault, J. P. An efficient strategy for the synthesis of circular RNA molecules. *Nucleic Acids Res.* **23**, 3064–6 (1995).
40. Beckert, B. & Masquida, B. Synthesis of RNA by in vitro transcription. *Methods Mol. Biol.* **703**, 29–41 (2011).
41. Deana, A., Celesnik, H. & Belasco, J. G. The bacterial enzyme RppH triggers messenger RNA degradation by 5' pyrophosphate removal. *Nature* **451**, 355–8 (2008).
42. England, T. E., Gumport, R. I. & Uhlenbeck, O. C. Dinucleoside pyrophosphate are substrates for T4-induced RNA ligase. *Proc. Natl. Acad. Sci. U. S. A.* **74**, 4839–42 (1977).
43. Thess, A. *et al.* Sequence-engineered mRNA Without Chemical Nucleoside Modifications Enables an Effective Protein Therapy in Large Animals. *Mol. Ther.* **23**, 1456–64 (2015).
44. Youn, H. & Chung, J.-K. Modified mRNA as an alternative to plasmid DNA (pDNA) for transcript replacement and vaccination therapy. *Expert Opin. Biol. Ther.* **15**, 1337–48 (2015).
45. Wolff, J. A. *et al.* Direct gene transfer into mouse muscle in vivo. *Science* **247**, 1465–8 (1990).
46. Okumura, K. *et al.* Bax mRNA therapy using cationic liposomes for human malignant melanoma. *J. Gene Med.* **10**, 910–7 (2008).
47. Zangi, L. *et al.* Modified mRNA directs the fate of heart progenitor cells and induces vascular regeneration after myocardial infarction. *Nat. Biotechnol.* **31**, 898–907 (2013).
48. Creusot, R. J. *et al.* A short pulse of IL-4 delivered by DCs electroporated with modified mRNA can both prevent and treat autoimmune diabetes in NOD mice. *Mol. Ther.* **18**, 2112–20 (2010).

-
49. Gonzalez, G., Pfannes, L., Brazas, R. & Striker, R. Selection of an optimal RNA transfection reagent and comparison to electroporation for the delivery of viral RNA. *J. Virol. Methods* **145**, 14–21 (2007).
 50. Kim, T. K. & Eberwine, J. H. Mammalian cell transfection: the present and the future. *Anal. Bioanal. Chem.* **397**, 3173–8 (2010).
 51. Suda, T. & Liu, D. Hydrodynamic gene delivery: its principles and applications. *Mol. Ther.* **15**, 2063–9 (2007).
 52. Karikó, K., Ni, H., Capodici, J., Lamphier, M. & Weissman, D. mRNA is an endogenous ligand for Toll-like receptor 3. *J. Biol. Chem.* **279**, 12542–50 (2004).
 53. Yamamoto, A., Kormann, M., Rosenecker, J. & Rudolph, C. Current prospects for mRNA gene delivery. *Eur. J. Pharm. Biopharm. Off. J. Arbeitsgemeinschaft für Pharm. Verfahrenstechnik e.V* **71**, 484–9 (2009).
 54. Human insulin receives FDA approval. *FDA Drug Bull.* **12**, 18–9 (1982).
 55. NCD Risk Factor Collaboration. Worldwide trends in diabetes since 1980: a pooled analysis of 751 population-based studies with 4·4 million participants. *Lancet* **387**, 1513–1530 (2016).
 56. World Health Day 2016: WHO calls for global action to halt rise in and improve care for people with diabetes. (2016). Available at: <http://www.who.int/mediacentre/news/releases/2016/world-health-day/en/>. (Accessed: 15th April 2016)
 57. Bottazzo, G. F. *et al.* In situ characterization of autoimmune phenomena and expression of HLA molecules in the pancreas in diabetic insulinitis. *N. Engl. J. Med.* **313**, 353–60 (1985).
 58. Ziegler, A. G. *et al.* Seroconversion to multiple islet autoantibodies and risk of progression to diabetes in children. *JAMA* **309**, 2473–9 (2013).
 59. Ziegler, A.-G. & Nepom, G. T. Prediction and pathogenesis in type 1 diabetes. *Immunity* **32**, 468–78 (2010).
-

60. Qi, M. Transplantation of Encapsulated Pancreatic Islets as a Treatment for Patients with Type 1 Diabetes Mellitus. *Adv. Med.* **2014**, 15 (2014).
61. Ziegler, A. G. *et al.* Primary Prevention of Beta-cell Autoimmunity and Type 1 Diabetes – The Global Platform for the Prevention of Autoimmune Diabetes (GPPAD) Perspectives. *Mol. Metab.* **5**, 255–62 (2016).
62. van Belle, T. L., Coppieters, K. T. & von Herrath, M. G. Type 1 diabetes: etiology, immunology, and therapeutic strategies. *Physiol. Rev.* **91**, 79–118 (2011).
63. Yaturu, S. Insulin therapies: Current and future trends at dawn. *World J. Diabetes* **4**, 1–7 (2013).
64. Agarwal, A. & Brayman, K. L. Update on islet cell transplantation for type 1 diabetes. *Semin. Intervent. Radiol.* **29**, 90–8 (2012).
65. Gefen-Halevi, S. *et al.* NKX6.1 Promotes PDX-1-Induced Liver to Pancreatic β -Cells Reprogramming. (2010).
66. Kojima, H. *et al.* Extrapancreatic insulin-producing cells in multiple organs in diabetes. *Proc. Natl. Acad. Sci. U. S. A.* **101**, 2458–63 (2004).
67. Hernan, R., Heuermann, K. & Brizzard, B. Multiple epitope tagging of expressed proteins for enhanced detection. *Biotechniques* **28**, 789–93 (2000).
68. Hopp, T. P. *et al.* A Short Polypeptide Marker Sequence Useful for Recombinant Protein Identification and Purification. *Bio/Technology* **6**, 1204–1210 (1988).
69. Terpe, K. Overview of tag protein fusions: from molecular and biochemical fundamentals to commercial systems. *Appl. Microbiol. Biotechnol.* **60**, 523–33 (2003).
70. Stacer, A. C. *et al.* NanoLuc reporter for dual luciferase imaging in living animals. *Mol. Imaging* **12**, 1–13 (2013).
71. Laios, E., Obeid, P. J., Ioannou, P. C. & Christopoulos, T. K. Expression

- hybridization assays combining cDNAs from firefly and Renilla luciferases as labels for simultaneous determination of two target sequences. *Anal. Chem.* **72**, 4022–8 (2000).
72. Matthews, J. C., Hori, K. & Cormier, M. J. Purification and properties of Renilla reniformis luciferase. *Biochemistry* **16**, 85–91 (1977).
73. Tannous, B. A., Kim, D.-E., Fernandez, J. L., Weissleder, R. & Breakefield, X. O. Codon-optimized Gaussia luciferase cDNA for mammalian gene expression in culture and in vivo. *Mol. Ther.* **11**, 435–43 (2005).
74. Hall, M. P. *et al.* Engineered luciferase reporter from a deep sea shrimp utilizing a novel imidazopyrazinone substrate. *ACS Chem. Biol.* **7**, 1848–57 (2012).
75. Germain-Genevois, C., Garandeau, O. & Couillaud, F. Detection of Brain Tumors and Systemic Metastases Using NanoLuc and Fluc for Dual Reporter Imaging. *Mol. Imaging Biol.* **18**, 62–9 (2016).
76. Tran, V., Moser, L. A., Poole, D. S. & Mehle, A. Highly sensitive real-time in vivo imaging of an influenza reporter virus reveals dynamics of replication and spread. *J. Virol.* **87**, 13321–9 (2013).
77. Hovhannisyan, R. H. & Carstens, R. P. Heterogeneous ribonucleoprotein m is a splicing regulatory protein that can enhance or silence splicing of alternatively spliced exons. *J. Biol. Chem.* **282**, 36265–74 (2007).
78. Geng, J. & Carstens, R. P. Two methods for improved purification of full-length mammalian proteins that have poor expression and/or solubility using standard Escherichia coli procedures. *Protein Expr. Purif.* **48**, 142–50 (2006).
79. Sonvilla, G. *et al.* FGF18 in colorectal tumour cells: autocrine and paracrine effects. *Carcinogenesis* **29**, 15–24 (2008).
80. *Creating Standard Curves with Genomic DNA or Plasmid DNA Templates for Use in Quantitative PCR.* (2003).

81. Kaushansky, A. *et al.* Malaria parasites target the hepatocyte receptor EphA2 for successful host infection. *Science* **350**, 1089–92 (2015).
82. Phua, K. K. L., Leong, K. W. & Nair, S. K. Transfection efficiency and transgene expression kinetics of mRNA delivered in naked and nanoparticle format. *J. Control. Release* **166**, 227–33 (2013).
83. Kreiter, S., Diken, M., Selmi, A., Türeci, Ö. & Sahin, U. Tumor vaccination using messenger RNA: Prospects of a future therapy. *Curr. Opin. Immunol.* **23**, 399–406 (2011).
84. Schoenberg, D. R. & Maquat, L. E. Regulation of cytoplasmic mRNA decay. *Nat. Rev. Genet.* **13**, 246–59 (2012).
85. Nigro, J. M. *et al.* Scrambled exons. *Cell* **64**, 607–13 (1991).
86. Kamimura, K., Abe, H., Suda, T., Aoyagi, Y. & Liu, D. Liver-directed Gene Therapy. *JSM Gastroenterol. Hepatol.*
87. Alsaggar, M. & Dexi, L. in *Gene Therapy and Cell Therapy Through the Liver: Current Aspects and Future Prospects* (eds. Terai, S. & Suda, T.) 185 (Springer, 2015).
88. Nishikawa, M. *et al.* Hepatocyte-targeted in vivo gene expression by intravenous injection of plasmid DNA complexed with synthetic multi-functional gene delivery system. *Gene Ther.* **7**, 548–55 (2000).
89. Turner, P. V, Brabb, T., Pekow, C. & Vasbinder, M. A. Administration of substances to laboratory animals: routes of administration and factors to consider. *J. Am. Assoc. Lab. Anim. Sci.* **50**, 600–13 (2011).
90. Karikó, K., Muramatsu, H., Keller, J. M. & Weissman, D. Increased Erythropoiesis in Mice Injected With Submicrogram Quantities of Pseudouridine-containing mRNA Encoding Erythropoietin. *Mol. Ther.* **20**, 948–953 (2012).
91. Hedrich, H. J. & Bullock, G. R. *The Laboratory Mouse*. (Elsevier Academic Press, 2004).

92. Baeshen, N. A. *et al.* Cell factories for insulin production. *Microb. Cell Fact.* **13**, 141 (2014).
93. Zheng, S., Ghitani, N., Blackburn, J. S., Liu, J.-P. & Zeitlin, S. O. A series of N-terminal epitope tagged Hdh knock-in alleles expressing normal and mutant huntingtin: their application to understanding the effect of increasing the length of normal Huntingtin's polyglutamine stretch on CAG140 mouse model pathogenesis. *Mol. Brain* **5**, 28 (2012).
94. Dey, A. *et al.* Loss of the tumor suppressor BAP1 causes myeloid transformation. *Science* **337**, 1541–6 (2012).
95. Brown, M. & Wittwer, C. Flow cytometry: principles and clinical applications in hematology. *Clin. Chem.* **46**, 1221–9 (2000).
96. Gonçalves, L. A., Vigário, A. M. & Penha-Gonçalves, C. Improved isolation of murine hepatocytes for in vitro malaria liver stage studies. *Malar. J.* **6**, 169 (2007).
97. K., G. N. *Insulin Receptor Positive T Cell Transgenic Mice and Implications for Type-1 Diabetes.* (ProQuest, 2011).
98. Despoix, N. *et al.* Mouse CD146/MCAM is a marker of natural killer cell maturation. *Eur. J. Immunol.* **38**, 2855–64 (2008).
99. Viegas, M. S., Martins, T. C., Seco, F. & do Carmo, A. An improved and cost-effective methodology for the reduction of autofluorescence in direct immunofluorescence studies on formalin-fixed paraffin-embedded tissues. *Eur. J. Histochem.* **51**, 59–66
100. Chen, C.-Y. A., Ezzeddine, N. & Shyu, A.-B. Messenger RNA half-life measurements in mammalian cells. *Methods Enzymol.* **448**, 335–57 (2008).
101. Blow, N. In vivo molecular imaging: the inside job. *Nat. Methods* **6**, 465–469 (2009).
102. Jacobs, F., Gordts, S. C., Muthuramu, I. & De Geest, B. The liver as a target organ for gene therapy: state of the art, challenges, and future perspectives.

- Pharmaceuticals (Basel)*. **5**, 1372–92 (2012).
103. Knook, D. L. & Sleyster, E. C. Isolated parenchymal, Kupffer and endothelial rat liver cells characterized by their lysosomal enzyme content. *Biochem. Biophys. Res. Commun.* **96**, 250–7 (1980).
104. Blouin, A., Bolender, R. P. & Weibel, E. R. Distribution of organelles and membranes between hepatocytes and nonhepatocytes in the rat liver parenchyma. A stereological study. *J. Cell Biol.* **72**, 441–55 (1977).
105. Do, H., Healey, J. F., Waller, E. K. & Lollar, P. Expression of factor VIII by murine liver sinusoidal endothelial cells. *J. Biol. Chem.* **274**, 19587–92 (1999).
106. Crowley, S. T., Poliskey, J. A., Baumhover, N. J. & Rice, K. G. Efficient expression of stabilized mRNA PEG-peptide polyplexes in liver. *Gene Ther.* **22**, 993–9 (2015).
107. McCaffrey, A. P. *et al.* Determinants of hepatitis C translational initiation in vitro, in cultured cells and mice. *Mol. Ther.* **5**, 676–84 (2002).
108. Wilber, A. *et al.* RNA as a source of transposase for Sleeping Beauty-mediated gene insertion and expression in somatic cells and tissues. *Mol. Ther.* **13**, 625–30 (2006).
